N64-10903

CR-52731

FINAL REPORT FOR

STUDY OF TOPSIDE SOUNDER FOR

MARS AND VENUS IONOSPHERES

FROM MARINER SPACECRAFT

by

T. Flattau and R. Donegan

1844-1

October 1963

Prepared for

National Aeronautics and Space Administration
Office of Space Sciences
Contract NASw-513

CUTLER ╱ HAMMER

AIRBORNE INSTRUMENTS LABORATORY
DEER PARK, LONG ISLAND, NEW YORK

CONTROL AIL/ DIVISION

FINAL REPORT FOR

STUDY OF TOPSIDE SOUNDER FOR

MARS AND VENUS IONOSPHERES

FROM MARINER SPACECRAFT

by

T. Flattau and R. Donegan

1844-1

October 1963

Prepared for

CUTLER HAMMER

TABLE OF CONTENTS

LIST OF ILLUSTRATIONS

ABSTRACT

This report analyzes the problems and solutions in sounding the topside of the ionospheres of Mars and Venus from a passing spacecraft. It shows that the pulse-ranging techniques traditionally used for ionospheric sounding are impractical in this application due to the high peak powers required. A recommended system configuration using a set of optimum techniques for performing the soundings that requires peak RF powers that are compatible with solid-state transmitters is described.

Transmission of an interrupted CW (50-percent duty cycle) RF pulse train that is small-angle phase modulated by a 150-cps tone is chosen as the optimum modulation. The distance to the reflecting layer of the ionosphere can then be determined by measuring the phase delay of the detected tone in the received signal.

A partial breadboard of the recommended system was constructed during the study to verify the suitability of the various techniques and their compatibility. The design specifications and details of the system components are discussed.

I. INTRODUCTION

This is the final report of a one-year study performed by Airborne Instruments Laboratory (AIL) for the NASA Office of Space Sciences under Contract NASw-513.

An experiment has been suggested for inclusion in the Mariner program to determine certain properties of the atmospheres of Mars and Venus through topside radio soundings of the planets' ionospheres. The objective of this study is to define a system that will accurately measure (50-km resolution) the distance from the spacecraft to the reflecting region of the ionosphere from a maximum range of 40,000 km at each of three sounding frequencies. All reflections are expected to occur within a 1,000-km band, requiring the system to resolve the reflecting region into 20 resolution elements. Observations of these topside reflections will provide a measure of the atmosphere's scale height and an estimate of its peak electron density.

The Central Radio and Propagation Laboratory (CRPL) of the National Bureau of Standards has performed a study of the scientific aspects and objectives of this experiment. The CRPL study has established the scientific model in which the experiment is to be performed and has recommended the use of 1, 2, and 5 Mc for the Mars sounding, and 4.5, 6, and 9 Mc for sounding Venus.

This report analyzes the engineering aspects of the problem and determines the system techniques that are optimum for performing this experiment in the expected space environment. This environment places certain constraints on the design of the ionosounder. Months will elapse between the time the flight is started and the time the planet is

approached and the soundings made. Thus, system reliability and simplicity are important requirements. The high cost of placing a pound of payload in the vicinity of the planet requires that the ionosounder weight be held to a minimum. Electrical energy consumption also must be minimized, since this is directly related to the weight of the needed electrical energy source. Solid-state components with their high reliability and low weight should be used wherever possible.

The Mariner spacecraft are expected to have planetary near-miss distances between 8,000 and 27,000 kilometers, and an approach velocity of 5 km/second. Topside soundings made over a three-hour interval during the fly-by require that the sounder operate from a maximum range between 12,000 and 40,000 km (Figure 1-1). This 40,000-km maximum range entails an extremely large path loss for radio sounding. The planetary sounder must, therefore, use techniques that make efficient use of the available electrical energy and that require peak transmitter powers for sounding that are compatible with solid-state devices.

The sections that follow analyze various techniques that could be used in the ionosounder, and recommend the optimum set. The remainder of the study describes the optimum system with its interfaces, and specifies its components in detail. It also describes the breadboard performance in both laboratory simulated soundings and as a bottomside sounder of the earth's ionosphere.

SPACECRAFT VELOCITY = 5 km

RANGE OVER
WHICH SOUNDINGS
WILL BE MADE

30,800 km

30,800 km

APPROXIMATE
SPACECRAFT
TRAJECTORY

40,000-km MAXIMUM
SOUNDING RANGE

27,000-km
MAXIMUM MISS
DISTANCE

8,950 km

12,000 km

8,000-km
MINIMUM
SOUNDING
RANGE

PLANET

R

$R_{MARS} \approx 3,000$ km

$R_{VENUS} \approx 6,000$ km
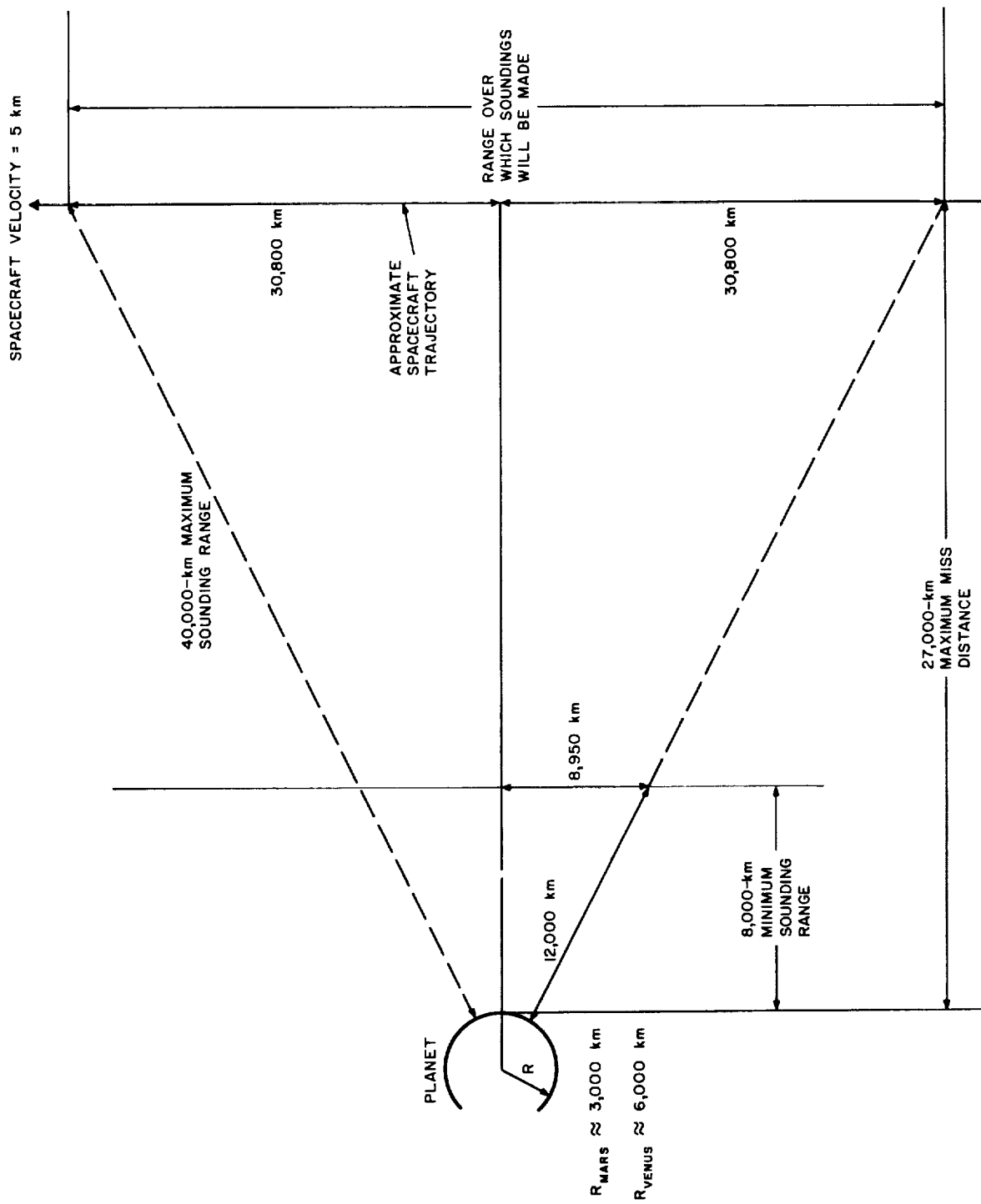
FIGURE 1-1.   SPACECRAFT NEAR-MISS TRAJECTORY

II. MODULATION

A. RECEIVER SIGNAL-TO-NOISE RATIO S/N

Appendix A derives the received S/N per cycle of bandwidth that would be present in a radio sounder subject to the cosmic noise of interplanetary space. Table 2-I gives these values (a sounding range of 40,000 km) for 1 watt of radiated power at various frequencies for Mars and for Venus.

TABLE 2-I

RECEIVED S/N PER CYCLE OF BANDWIDTH AT 40,000 KM

1 watt of radiated power

Isotropic antennas

Specular loss-less reflecting ionosphere with
no mode splitting

Frequency (Mc)	S/N (db) Mars	Venus
1.0	3.4	8.0
2.0	4.3	8.9
4.5	5.3	9.9
5.0	5.5	10.1
6.0	5.7	10.3
9.0	6.2	10.8

B. PULSED MODULATION

The use of conventional radar-pulsing techniques requires a pulse width of $\frac{2R}{c}$ where R is the desired resolution in meters and C is 3×10^8 meters/second, the velocity of light. The required radar receiver bandwidth is the

reciprocal of the pulse width. Thus, 50-km resolution requires a bandwidth of $\dfrac{3 \times 10^8}{2 \times 5 \times 10^4} = 3 \times 10^3$ cps, and results in a S/N decrease of 34.8 db from that for a 1-cps bandwidth.

The 3.4-db S/N shown in Table 2-I for 1-Mc soundings of Mars would be reduced to -31.4 db for a single pulse sounding. A radiated power of 44,500 watts (31.4 db + 15 db over 1 watt) is required to produce the necessary S/N of about 15 db. This power is far above what can be obtained from present solid-state devices.

Integration of the signal returns would reduce the transmitter power requirement, but is impractical due to the thousands of pulse returns that would have to be integrated over many seconds of time to produce the necessary S/N increase.

C.   PULSE MODULATION WITH CODING

Proper coding (intra-pulse modulation and multiple pulse groups) is a method frequently used to reduce the peak power requirements of a pulsed radar through spreading of the radiated energy in either frequency or time, or both. However, a peak power reduction of at least three orders of magnitude is needed to reduce the power requirement to an acceptable level. Frequency compression and time-delay networks with this capability are not practical for this system due to their physical size.

D.   INTERRUPTED CW

The requirement of keeping peak power levels within a practical limit (about 100 watts) requires the use of a high-duty-cycle transmission of which CW is the upper limit. It also indicates that narrow-band reception is necessary.

The maximum round-trip signal attenuation for a 1-Mc signal is about 150 db at 40,000 km range (Appendix A).

This requires that the transmitter be off during the time of the expected signal return to avoid having the transmission overload the receiver. No practical transmit-receive isolation will accommodate the 150-db signal ratio. Thus, a 50-percent transmission duty cycle is the practical upper limit for the transmitter.

E. TYPE MODULATION

With the duty cycle now chosen, the choice between amplitude and angle modulation remains to be made. There is about a 5 to 1 variation in sounding range expected, which would produce about a 28-db received signal strength variation. The use of amplitude modulation would require an automatic gain control loop in the receiver to avoid the possibility of loss of modulation through receiver overloading. Angle modulation requires the use of a simple limiter in the receiver and permits a receiver design that can tolerate a wide variation in its gain. An angle-modulation transmitter is also much simpler and smaller than an amplitude-modulation transmitter of equal efficiency.

Small index angle modulation requires no more bandwidth than amplitude modulation and is the method of modulation best suited for this system. Large index angle modulation provides an S/N enhancement at high S/N, but is not considered desirable in this application due to the increase in its S/N threshold that occurs with the increasing S/N enhancement at higher modulation indices.

F. MODULATING SIGNAL CHOICE

The angle-modulated signal may be represented by $S(t) = A \cos \left[\omega_c t + \phi(t) \right]$ during its time of transmission.

where

A = Signal amplitude

ω_c = Carrier radian frequency

t = time

$\emptyset(t)$ = Modulating signal

The modulating signal is to be optimized, so that the system can detect the required measurement data with the minimum expenditure of energy. With the type of modulation selected being small-angle modulation, minimum energy expenditure is synonymous with minimum bandwidth.

CRPL has indicated that the reflecting region of the planetary ionospheres for the sounding frequencies used will be within a 1000-km band, and that the soundings should be resolved to within 50 km.

Thus, the sounder must resolve the reflecting range into one of 20 possible elements during each sounding interval, which is a measure of the system's information capacity. An increase of this capacity from the minimum of one in 20 requires that either system bandwidth or S/N be higher than the minimum.

The measurement of range with radio waves is actually a measurement of the round-trip propagation time. Thus, in effect, a clock in the sounder must be synchronized with the transmitted modulation, $\emptyset(t)$, so that it can measure the elapsed propagation time. The time delay between the sounder clock $\emptyset(t)$ and the received $\emptyset(t)$ is the desired measurement that must be resolved into one of 20 elements. $\emptyset(t)$ must be chosen to allow the making of this measurement with the minimum expenditure of bandwidth.

Two usable forms of $\emptyset(t)$ that are simple to implement are a linear frequency sweep, $\emptyset(t) = K_1 t^2$ radians and a sinusoidal form $\emptyset(t) = K_2 \sin \omega_m t$ radians, where both are periodic with a period equal to the round-trip propagation time for 1000 km. The sinusoidal modulation signal is optimum as it requires a bandwidth considerably less than the

linear sweep, and, in fact, requires the minimum bandwidth
of any modulation signal.

G. MODULATION SIGNAL SPECIFICATIONS

Small-angle phase modulation of the interrupted
CW sounding frequency with a sinusoid is considered the opti-
mum modulation for this system. An analysis of the specifi-
cations for this modulation follows.

1. TRANSMITTER "ON" TIME

It is desirable that the transmitter, when at maxi-
mum sounding range, be turned off simultaneously with the
arrival of the leading edge of the reflected signal. This
coupled with the 50-percent duty cycle provides maximum use
of the transmitted energy. The 40,000-km range corresponds
to about a 250-msec round-trip time. Thus, the transmitter
on-off rate is 2 cps.

2. MODULATION SINUSOID

The period of the sinusoidal modulation should cor-
respond to the 1000-km band of range within which the measure-
ment is to be resolved. The round-trip propagation time across
1000 km is $\frac{1}{150}$ second, so the sinusoid frequency is 150 cps.

The stability requirement for the 150-cps sinusoid
is determined by the accuracy required in knowing the differ-
ence between the sounding ranges for any two of the sounding
frequencies. The modulation phase delay due to the propaga-
tion time is measured directly by the sounder, and this delay
is then related to a delay time (or distance) by converting
the fraction of 2π radians occupied by the phase delay to that
same fraction of the modulation period. Thus, for a measured
phase-delay difference of ϕ radians between two soundings,

and a modulation period T, the delay-time difference, t, represented by the measurement is:

$$t = T \times \frac{\emptyset}{2\pi}$$

and

$$\frac{\Delta t}{T} = \frac{\Delta T}{T} \times \frac{\emptyset}{2\pi}$$

where Δt is the resultant error in the delay time between any two measurements caused by an error ΔT being added to the design modulation period T. The desired resolution element is 50 km, and the modulation period corresponds to 1000 km. If the measurement error is arbitrarily allowed to reach 1/4 of a resolution element in the worst case when $\emptyset$ approaches 2π, then

$$\frac{\Delta T}{T} = \frac{1/4 \times 50}{1000} = \frac{1}{80}$$ or 1.25-percent frequency stability, since the times are directly related to distances.

A stronger criteria for modulation stability occurs in the short-term frequency drift. A change in the modulation period during the course of a 1/4 second transmission will result in a change in the measured delay time that increases as the sounding range increases. If the sounding range is d meters and the round trip propagation time is $2 \times \frac{c}{d}$ seconds, where c is the average propagation velocity:

then $\frac{2c}{d} = nT + t$.

Where

      n = Number of complete modulation periods

      T = Design modulation period

      t = Measured delay time

ΔT = Change in modulation period

Δt = Change in measured delay time

If d and n remain constant

$$nT + t = n(T + \Delta T) + (t + \Delta t)$$

$$\frac{\Delta t}{T} = -n \frac{\Delta T}{T}$$

Thus, if the measurement is to change by less than 1/4 of a resolution element at the maximum sounding range of 40,000 km,

$$\left| \frac{\Delta T}{T} \right| \leq \frac{1}{40} \times \frac{1/4 \times 50}{1000}$$

$$\left| \frac{\Delta T}{T} \right| \leq 3.12 \times 10^{-4}$$

Thus, the modulation frequency must drift less than 0.031 percent during the time of sounding of any two frequencies.

3. MODULATION INDEX

The choice of the modulation index is based on minimizing the required receiver bandwidth, while still maintaining adequate side-band power for the measurement.

The modulated signal may be represented as

$$S(t) = A \sin (2\pi f_c t + m \cos 2\pi f_m t)$$

$$S(t) = A \{J_o(m) \sin 2\pi f_c t +$$

$$J_1(m) [\cos 2\pi(f_c + f_m)t + \cos 2\pi(f_c - f_m)t] + \}$$

f_c = Sounding frequency

f_m = Modulation frequency

m = Radian depth of angle modulation

J_n = Bessel function, first kind, n^{th} order

Inspection of $J_o(m)$ and $J_1(m)$ indicates that if $m = \frac{\pi}{4}$,

$$J_o\left(\frac{\pi}{4}\right) = 0.852$$

$$J_1\left(\frac{\pi}{4}\right) = 0.362$$

and that

$$\left[J_o\left(\frac{\pi}{4}\right)\right]^2 = 0.726 =$$

the fraction of transmitted power in the carrier,

$$2\left[J_1\left(\frac{\pi}{4}\right)\right]^2 = 0.262 =$$

the fraction of the transmitted power in the first sidebands.

Thus, all but 1 percent of the signal power is in the carrier and first pair of sidebands. In addition, adequate power resides in the sidebands for the phase-delay measurement.

III. SIGNAL DETECTION

A. RECEIVED SIGNAL CHARACTERISTICS

The received signal will be pulses of carrier that are angle modulated at 150 cps. It will be modified from the transmitted signal as follows:

1. The received pulse width will be directly proportional to the sounding range:

$$\text{Received pulse width} = \frac{\text{Range} \times 2}{\text{Propagation velocity}}$$

The width at the 8000-km minimum range will be

$$\frac{1.6 \times 10^7}{3 \times 10^8} = 53 \text{ msec}$$

2. Carrier and modulation frequencies will be doppler shifted (Appendix B). The modulation doppler shift will present no problem due to its small magnitude, but the carrier frequency shift is significant. Maximum doppler shift in cps = Sounding frequency (Mc) × 24. Thus, at the maximum sounding frequency of 9 Mc for Venus, the maximum doppler shift will be +216 cps. The maximum doppler rate at this frequency will be 0.14 cps/sec.

3. The signal return will have some spectrum spreading due to perturbations in the reflecting ionosphere. The opinion of CRPL is that this will be generally less than 1 cps.

4. The S/N per unit bandwidth is given in Appendix A and is tabulated for different frequencies in Section II-A.

B. SIGNAL DETECTION TECHNIQUES

1. DISCRIMINATOR

The simplest efficient detector for angle modulation is a discriminator. The equivalent noise bandwidth

for such a detection system is related to the required
receiver IF bandwidth and the post-detection bandwidth. The
post-detection bandwidth required is low (less than 1 cps),
but the receiver bandwidth needed is the sum of the maximum
bidirectional doppler shift ($\pm$216 cps), the modulation side-
bands (300 cps), and the expected system frequency drift.
This sum is 1 kc. Combining the receiver IF and the post-
detection bandwidths yields an equivalent noise bandwidth
that produces a system sensitivity far poorer than what can
be obtained with a phase-lock loop.

2. PHASE-LOCK LOOPS

The phase-lock loop is the detection system that is
best suited to the parameters of the sounding system for
demodulating the received signal. It can track the carrier
doppler thus acting as a tracking filter with a low equivalent
noise bandwidth. Much literature exists (references 1 through
9) describing and analyzing the operation of this detection
system. Appendix C shows a block diagram of such a loop and
describes the relationships between its important parameters.

C. SOUNDER SIGNAL DETECTOR

1. BANDWIDTHS

The receiver bandwidth required to accommodate
doppler shift, modulation sidebands, and system drift is 1 kc.
The maximum bandwidth required by each of the signal spectral
components (carrier and one pair of sidebands) is fixed at
1 cps by the maximum assumed perturbations in the reflecting
ionospheres. The optimum detection process should make use
of this narrow bandwidth requirement.

A phase-lock loop will remain locked on the carrier
signal, if the S/N in its equivalent noise bandwidth is
greater than zero db (reference 9). About 4 db is needed to
reliably acquire the signal. The optimum loop of Appendix C

3-2

has a two-sided noise bandwidth about 6.66 times the loop 3-db (information) bandwidth. Thus, using a 3-db loop bandwidth of 1 cps will provide a phase-lock loop S/N greater than the IF S/N by the ratio of the IF bandwidth (1 kc) to the loop noise bandwidth (6.66 cps), or 21.8 db. A minimum IF carrier S/N requirement of (average) 4 db - 21.8 db = -17.8 db (-14.8 db pulse S/N at maximum range because of 50-percent duty cycle) results when the 4-db S/N is required for signal acquisition.

The phase-lock loop performs a synchronous detection of the received signal, yielding the 150-cps modulation tone for measurement. A more detailed analysis of the signal detection process follows.

2.   PHASE-LOCK LOOP

The received signal has been specified as having a maximum duration of 250 msec when the sounding range is maximum. Turning the receiver on, also for 250 msec, during the expected signal return time tends to match the receiving system to the signal and provides a non-zero input to the phase-lock loop for 50 percent of the time, with zero input during the remainder. The use of an ideal integrator for the loop low-pass filter will cause the loop signals to be invariant during the receiver off-time. This permits the loop analysis at the maximum range to be the same as for a CW system with the time scale halved, and the S/N 3 db less than the pulse S/N.

The low-pass filter shown in Appendix C is equivalent to an ideal integrator in this respect, if it is electrically disconnected from the loop during receiver off-time, thus avoiding its discharging.

3. VARIABLE DOPPLER SHIFT PROBLEMS

Soundings are to be made on each of three frequencies during a planetary fly-by. The switching from one sounding frequency to another will cause a change in the doppler shift due to its direct dependence on frequency. This change would require a costly time and energy consuming signal reacquisition every time, unless use is made of the known relationship between the doppler shifts at each frequency. This may be done by generating the VCO signal in the phase-lock loop for each of the sounding frequencies, so that the doppler component of the VCO frequency will vary by the same factor as the change in the sounding frequency.

This can be accomplished by selectively attenuating the control voltage to the VCO, or by a frequency synthesis procedure. Although it requires more components, the latter is most desirable from the viewpoint of accuracy and circuit practicability.

IV. DATA MEASUREMENT

A. OBJECTIVE

The objective of the measurement is to obtain the round-trip propagation time of the sounding signals. This time is observable as a phase shift in the detected 150-cps modulation tone. Thus, the required measurement is the phase shift in the 150-cps tone.

B. CLOSED-LOOP SERVO

A closed-loop servo may be used to determine the phase shift. This would operate by sensing the phase difference between the transmitted and received modulation tones in a phase comparator, and using this difference to control a variable phase shifter that alters the phase of the transmitted tone that is applied to the comparator. This process continues until the phase difference is brought to a null, and the error voltage required to produce this null is indicative of the total phase that was shifted. The phase shifter may be mechanical or electronic.

This closed-loop technique requires a phase detector, amplification of the difference signal, and the variable phase shifters. The component complexity makes this technique undesirable.

C. OPEN-LOOP PHASE MEASUREMENT

An open-loop phase difference measurement may be made using a simple phase detector.

The simplest phase detectors produce an output voltage that is the cosine of the phase angle being measured. This form repeats itself every 180 degrees of phase shift.

However, the use of two simple phase detectors operated in quadrature provides a unique measurement of phase over 360 degrees. In this case one detector will indicate the sine of the angle, and the other the cosine. Taking the tangent of the phase angle as being equal to the ratio of the first output voltage over the second will also make the measurement independent of changes in the demodulated tone amplitude due to variations in S/N.

D.   DATA SIGNAL

The phase-lock loop synchronously demodulates the received sounding signal. The spectrum of this detected signal contains the 150-cps tone with sidebands consisting of the 2-cps pulse-repetition frequency (PRF) harmonics clustered about it. As the received signal pulses become narrower at reduced sounding ranges, the amplitude of the pulses will increase due to the lower path loss; however, the fraction of the signal energy lying in the sidebands will increase inversely with the pulse width, leaving a smaller portion of the total energy in the 150-cps tone. This may be written as:

$$E_{tone} \approx P_{pulse} \times T_{pulse}$$

where

$\quad\quad E_{tone}$ = energy in 150-cps tone,

$\quad\quad P_{pulse}$ = peak power of received signal pulse,

$\quad\quad T_{pulse}$ = pulse width

$\quad\quad\quad\quad L$ = sounding range,

$\quad\quad P_{pulse} \approx \dfrac{1}{L^n}$,

$\quad\quad T_{pulse} \approx L$,

$\quad\quad E_{tone} \approx \dfrac{1}{L^{(n-1)}}$.

Since n varies with range between 2 and 4 (Appendix A),
E_{tone} will increase as L decreases. Thus the energy in the
tone that is available for the phase measurement increases
at the shorter sounding ranges.

E. DATA SIGNAL/NOISE

Section III-C(1) derives -14.8 db as the minimum
carrier S/N in the 1-kc wide IF that will provide the 4-db
S/N threshold required in the phase-lock loop for signal
acquisition. Section II-G, F(3) shows that the modulation
sideband power is 0.262 of the total, or -5.8 db. Thus, if
the unmodulated signal present in the receiver during signal
acquisition has an IF S/N of -14.8 db, the modulation side-
band S/N will be -14.8 db and -5.8 db = -20.6 db. The detec-
tion process will yield a data S/N during the received pulse
of -17.6 db, a 3-db improvement due to coherent adding of
sideband power, in a 500-cps noise bandwidth. In the interest
of phase-measurement sensitivity, it is desirable to raise the
S/N by filtering. Practical considerations of achievable
selectivity indicate that a 10-cps noise bandwidth (3-db band-
width of 6.4 cps) filter is a good choice at the 150-cps
center frequency. This filtering will raise the minimum pulse
S/N by $\frac{500}{10}$ = 50 or 17 db to -0.6 db.

The presence of the maximum duty cycle of 50 percent
can be considered as decreasing the effective S/N by 3 db from
the peak S/N. The justification for this is the same as used
in Section III-C(2) for the phase-lock loop. That is, half
of the signal energy at the input to the phase detector exists
in the pulse sidebands. Thus the minimum effective signal
energy to noise energy at the phase-measurement input is 3 db
less than -0.6 db or -3.6 db in a 10-cps noise bandwidth
centered about 150 cps.

Appendix A shows that the required measurement S/N to provide the 50-km resolution is about 15 db. Thus an additional S/N enhancement of 15 + 3.6 db = 18.6 db is required after the phase measurement.

An efficient and easily realized post-detection S/N enhancement occurs when the detected signal is passed through a filter whose frequency response has the same form as the signal's spectrum. The measurement signal is a series of rectangular pulses that have a 50-percent duty cycle at maximum sounding range, and an amplitude depending on the measured phase. Using post-detection integration of this pulse train for a time $2t_o$, can be considered as integrating a single pulse of the same S/N and length $2t_o$. The effect on the S/N due to the 50-percent duty cycle has been taken into account by the 3-db S/N loss at the phase measurement.

Thus the equivalent signal spectrum being integrated is:

$$F(\omega) = 2A\, t_o\, \frac{\sin t_o \omega}{t_o \omega}$$

The Fourier integral of a pulse of amplitude A and width $2t_o$.

The filter that most closely matches this signal is an integrator that is "dumped" after time $2t_o$ and has the following impulse response:
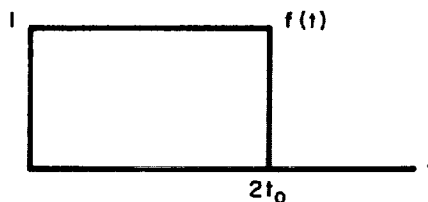
The Fourier integral of this impulse response is the effective frequency response of the filter and is:

$$H(f) = 2t_o \frac{\sin 2\pi t_o f}{2\pi t_o f}$$

The equivalent rectangular noise bandwidth (Hanson bandwidth) of this filter

$$B_n = \int_o^\infty \left| \frac{H(f)}{H(o)} \right|^2 df$$

and

$$B_n = \int_o^\infty \frac{\sin^2 2\pi f t_o}{(2\pi f t_o)^2} df$$

$$B_n = \frac{1}{4t_o} \text{ cps}$$

The S/N improvement provided by this integration process is approximately the ratio of the one-sided video noise bandwidths before and after integration or $\frac{5}{B_n} = 20t_o$.

Appendix D shows that an ideal integrator is approximated by an RC filter, when RC is large compared with the effective integration time. It indicates that the integration efficiency of an RC filter where $RC = t_o$ is within 0.3 db of the ideal integrator.

The actual signal being integrated is a 50-percent duty cycle train of pulses present for a time $2t_o$. Thus the RC integration requires a "holding" device to freeze the

integrated voltage during the "no pulse" time for the efficiency to be evaluated on the basis of t_o integration time instead of the actual time $2t_o$.

The integration S/N improvement is 20 t_o within 0.3 db for RC = t_o, and the required S/N improvement is 18.6 db, a ratio of 72. Thus 20 $t_o \approx$ 72 and t_o = 3.6 seconds, and the actual required integration time is 7.2 seconds.

The minimum IF carrier S/N	-14.8 db	
Decrease in power due to modulation:	-5.8 db	
Increase due to coherent adding of sidebands in detection process:		+3.0 db
Increase due to 10-cps filtering:		+17.0 db
Decrease due to 50 percent duty cycle:	-3.0 db	
Increase due to post-detection integration of 7.2 seconds:		+18.6 db
Totals:	-23.6 db	+38.6 db

and measurement = 15 db S/N

V. RF SIGNAL GENERATION

A. REQUIREMENTS

The Mars and Venus sounders should share as many common elements as possible. Therefore, the sounder should be capable of operating on the six sounding frequencies with a minimum of component switching. A superheterodyne receiver with six pairs of sounding and local-oscillator frequencies best satisfies this requirement. The frequency drift of the difference of each pair must be kept to less than ± 150 cps to avoid placing the modulated IF signal outside the IF pass band.

B. FREQUENCY GENERATION

The most straightforward method of stable frequency generation is to have a pair of crystal oscillators for each sounding frequency. An alternative method, shown in the following sketch, is to have two stable oscillators F_T and F_R, which remain in use for all of the soundings, and whose frequency difference $F_T - F_R$, is the IF of the receiver. Different sounding frequencies, $F_T - F_X$, with their proper local oscillator (LO) frequencies, $F_R - F_X$, can be selected by heterodyning a third frequency, F_X, with the first two.
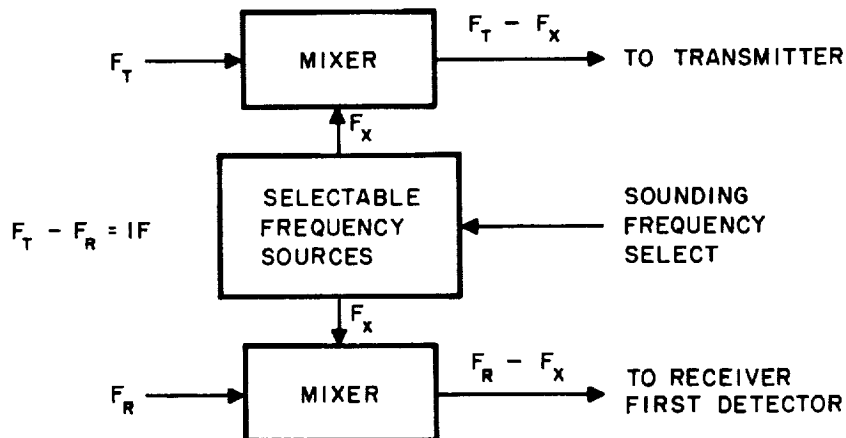
The latter method has the advantage of greater simplicity, flexibility, and uses fewer components unique to each sounding frequency.

C. <u>MODULATOR</u>

Small-angle phase modulation at 150 cps is required at each sounding frequency. The frequency generation method of the preceding section (B) is ideally suited for the placement of a phase modulator between the F_T source and the upper mixer. Angle modulation at frequency F_T is unaffected by the mixing process and will be the same at all of the sounding frequencies.

True phase modulation of F_T with a variable phase shifting network is recommended in contrast with frequency modulating the F_T source. This procedure will produce the greater frequency stability.

VI. SIGNAL ACQUISITION

Section III-C(1) described a phase-lock loop in the signal detection system of the sounder and its need to acquire the received signal. The reasons for the acquisition requirement are:

1. System frequency drift,
2. Doppler shift of received signal.

The frequency drift of concern here is the drift in the difference of the transmit and the local-oscillator frequencies. Stable crystal oscillators will limit this to ± 150 cps.

The doppler shift will depend on the spacecraft motion relative to the planet being sounded and the sounding frequency; this varies between ± 24 cps at 1 Mc, and ± 216 cps at 9 Mc for a spacecraft velocity of 5 km/sec at the maximum sounding range of 40,000 km.

Acquisition will be accomplished most efficiently by dividing it into the two parts of system drift and doppler shift.

The system drift can be removed without turning the transmitter on, by allowing a small leakage to occur between the sounding-frequency generator and the receiver. However, the doppler acquisition will require the presence of a reflected signal and no perceptible leakage.

The acquisition procedure will consist of sweeping the VCO in the phase-lock loop in two stages; the first will remove the system drift and the second will remove doppler shift. Both stages will use the same maximum sweep rate (reference 8) of twice the loop 3-db bandwidth per second (2 cps/

second), and the completion of the first stage will signal the start of the second. (No modulation will be used during acquisition so as to increase carrier signal strength and to avoid locking onto the side bands.) Acquisition in both stages will be indicated by the output of a phase detector, operating in quadrature with the phase-lock loop phase detector, having exceeded a threshold. This will signal the stopping of the VCO sweep, the turning on of the modulation, and the start of sounding.

Acquisition will require a maximum of 150 seconds during the drift acquisition, and a maximum varying between 24 seconds and 216 seconds for doppler as the sounding frequency is increased from 1 to 9 Mc.

VII. ANTENNAS, MATCHING NETWORKS, AND POWER AMPLIFIERS

There are several types of antennas that theoretically meet the requirements for the Mars and Venus flights. The antenna must have a large operating size with a small storage size and be lightweight. Furthermore, it must be simple because, in general, the more complex the antenna shape becomes, the more problems will arise in packaging and erecting.

A dipole antenna is recommended for both flights because of its comparative simplicity and light weight. It consists of two arms fed at the center. These arms can be projected out of opposite sides of the vehicle to the required size using either erection or inflatable techniques. From the standpoint of efficiency and impedance properties, the total length of the dipole ideally should be about one-half wavelength long at the frequency of operation. Since there are three frequencies involved, this would mean three separate antennas and would increase the weight, size, and complexity of the system. Since the wavelengths at the frequencies being used are so large, it would be advantageous mechanically and from the standpoint of weight to use less than a half wavelength dipole for two of the frequencies. The problem is, however, as the size of the dipole decreases, the resistance decreases rapidly whereas the reactance increases rapidly. For example, for a dipole about one-eighth wavelength in length, the resistance is about 2.5 ohms and the reactance approximately -j 1800 ohms. When this impedance is matched with a reactance of +j 1800 ohms, the resistance in this matching section may be of the order of 18 ohms (assuming a coil Q of 100), which means dissipating about 9 db of the available power in the matching section.

In addition, as the length of the antenna is changed, the antenna goes through several resonances (purely resistive) in which the problem is to match the resistance to the characteristic impedance of the feed line. The resonances occur approximately at multiples of one-half wavelength.

It is possible to operate the dipole up to a length of about 1-1/4 wavelengths. As 1-1/2 wavelengths is approached, however, the radiation pattern deteriorates into a multi-lobed pattern.

The dipole can be implemented using either erectable or inflatable techniques. An erectable technique would consist of some method of mechanically extending the arms out from the vehicle. This can be done by folding the arms like a carpenter's rule--that is, winding the arms on a spool or some other means. The inflatable technique would consist of two long metallized flexible tubes that would be inflated to their full length. These tubes should then be rigidized in some manner and evacuated. If they were not evacuated, then a hole punched in them would cause gas to escape and possibly cause the arms (or the vehicle) to change attitude. At this time, from the standpoint of reliability, minimum weight, and proven performance, it seems that the erectable type such as manufactured by DeHavilland and being used by AIL on the Topside Sounder (S-48 satellite) is the most logical choice. This consists of a metal strip wound on a spool. As the metal strip is unwound from the spool, it forms into a tubular shape (about 1/2 inch in diameter).

The exact point in transit when this antenna should be erected is subject to some discussion. However, some general rules can be pointed out at this time. The first rule should be that the antenna be erected after all major attitude or course corrections have been made. Since the dipoles con-

sist of relatively long and thin arms protruding from the vehicle, any violent maneuvers may tend to deform these arms or wrap them around the vehicle. Three other events that could occur to limit the success of the flight are:

1. Damage to the antenna (in extended position),

2. Failure to erect,

3. Loss of command ability.

The time of erection would then be a compromise. Erecting the antenna long before expected use would leave it vulnerable to damage, though the probability of damage is slight due to its small silhouette. However, if it fails to erect, there must be adequate time to try to erect it with some backup system. Also, it must be erected at a time when the probability of receiving and carrying out command signals is high.

The antenna length is determined practically by overall weight considerations, and the requirements set by the state of the art of the high-power, high-frequency transistors in the power amplifier. For the Mars mission, if a dipole pole length of 30 feet is used, a matching network loss of 20 db will result at 1 Mc (coil Q assumed to be 100). Thus, the power amplifier would be required to generate a power of 2000 watts to provide 20 watts of radiated power (the power necessary to provide adequate S/N). This power output cannot be obtained with transistors that are currently available. However, if a dipole with 60-foot poles is used, the power amplifier need generate only 224 watts. This output power can be obtained using two transistors (2N1900) in parallel. Using the required radiated powers for the Mars flight of 16 watts for 2 Mc and 12.3 watts for 5 Mc and assuming: (1) a transmitter on-time per frequency per sounding of 8 seconds, (2) a total of 100 sounding cycles, and

(3) a power amplifier efficiency of 80 percent. It can be shown that 76.2 watts/hour of energy will be required for the transmitters for the Mars mission. Assuming a figure of 30 watts/hour per pound for silver-zinc batteries, the required battery weight is then 2.54 pounds. The total weight of the 60-foot DeHavilland antenna is 5.0 pounds. Thus, for a 60-foot dipole the total weight of the batteries and antenna is 7.54 pounds. Using a similar analysis and using DeHavilland dipoles whose pole lengths are 100 feet, a total weight of antenna plus batteries can be shown to be 8.6 pounds. From the standpoint of weight, the best antenna length for the Mars mission is 60 feet. When the preceding criteria was used for the Venus mission, a 30-foot antenna system was found to be the most desirable.

The anticipated antenna matching losses for 30-foot and 60-foot dipoles are shown in Figure 7-1 as a function of frequency.
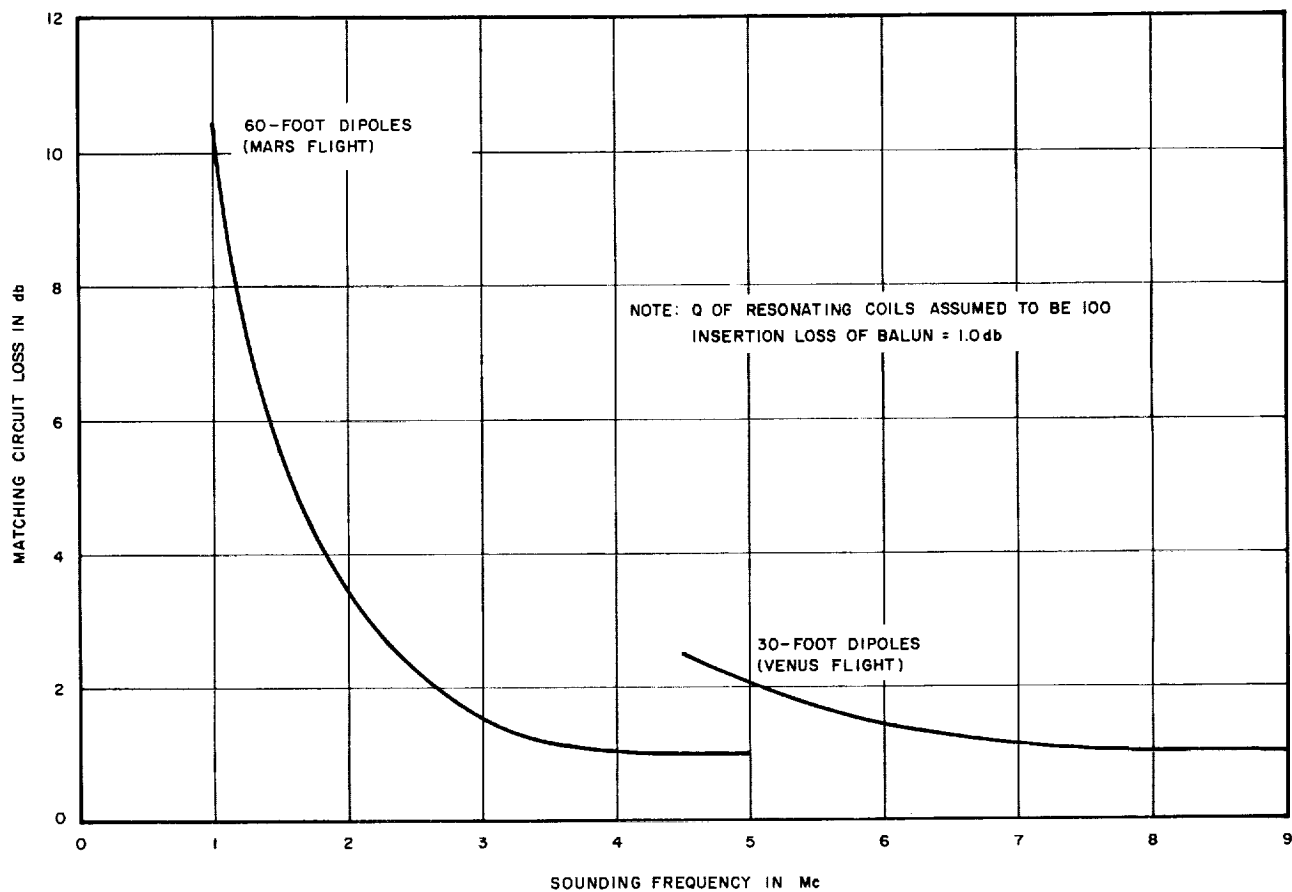
FIGURE 7-1. ANTENNA MATCHING NETWORK INSERTION LOSSES

VIII. TIMING AND CONTROL

The ionosounder has certain timing and control requirements. These are:

1. Antenna erection,
2. Power turn on,
3. Start and stop sounding,
4. Signal acquisition:
    (a) System frequency drift,
    (b) Doppler frequency shift,
5. Sounding PRF,
6. Sounding frequency sequencing.

Functions 1, 2, and 3 are of a command nature and can be satisfied via the command link or vehicle timer, or most desirably by both.

Function 4 is initiated by the start of sounding and continues until sounder sensors indicate its completion. Figure 8-1 shows its logic.

The sounder PRF and frequency sequencing signals are both low frequency (2 cps and maximum of 1/24 cps, respectively). The large size of components required in a 1/24 cps oscillator indicates that both signals should be derived from a single oscillator through binary division. Figures 8-2 and 8-3 show the binary countdown and logic required to perform this function.

FIGURE 8-1. SIGNAL ACQUISITION CONTROL
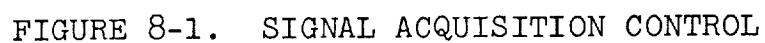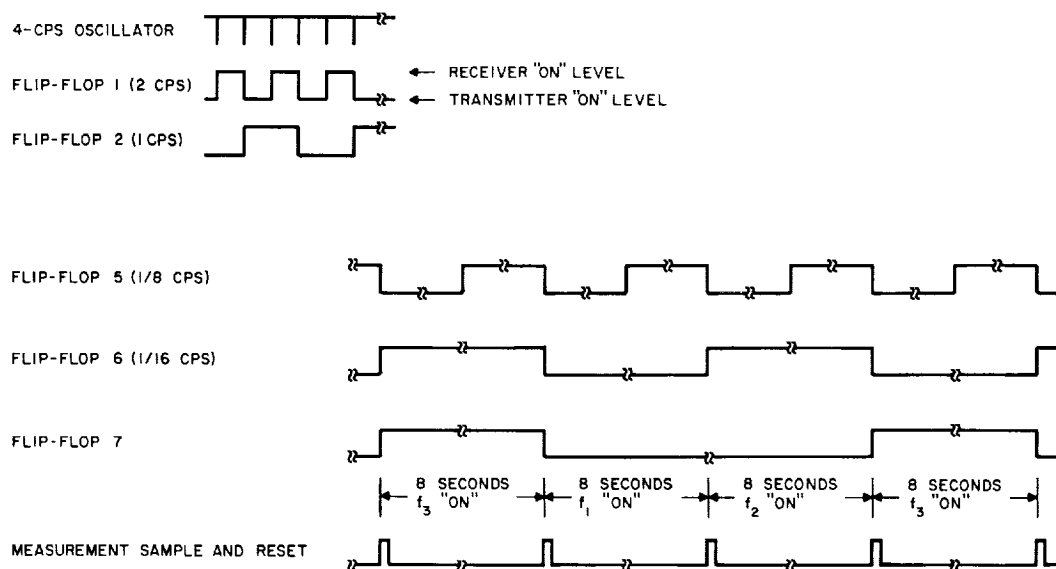
FIGURE 8-2. MEASUREMENT TIMING WAVEFORMS
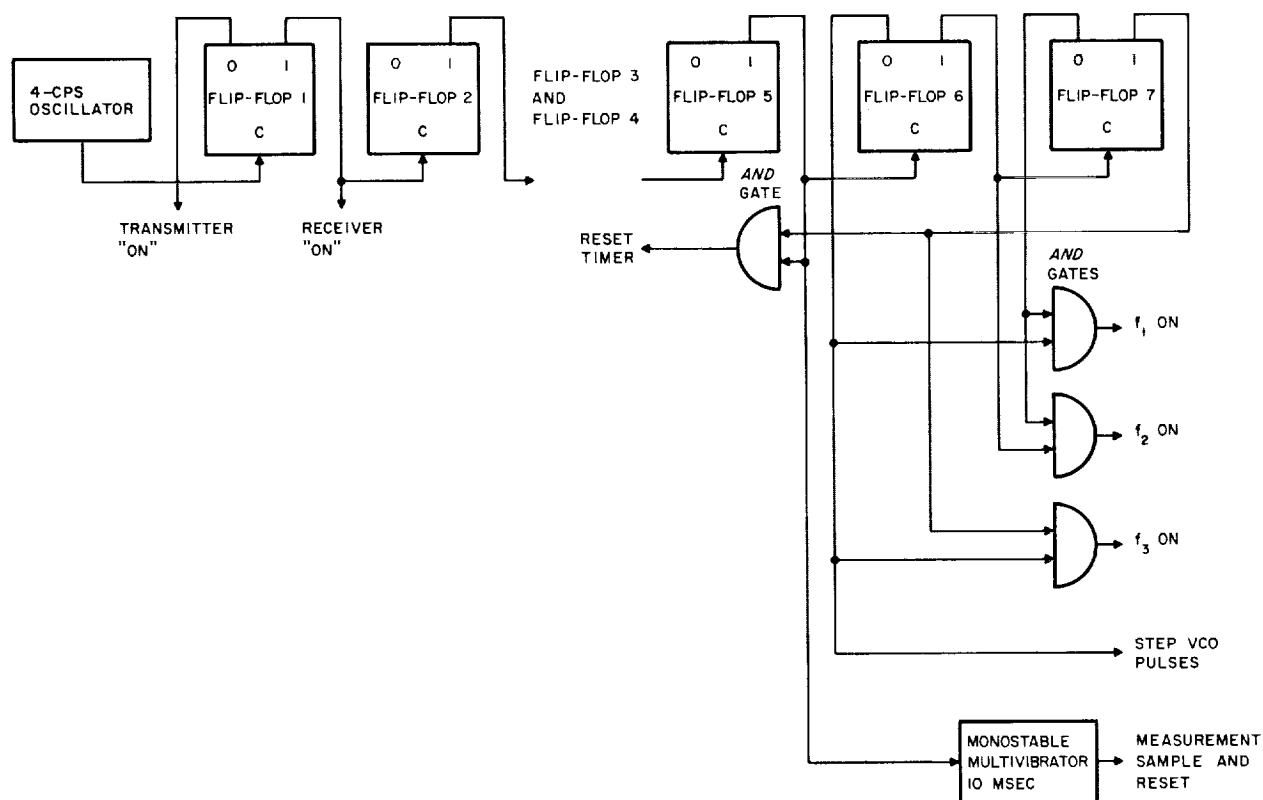
FIGURE 8-3. MEASUREMENT TIMER LOGIC

IX. IONOSOUNDER SYSTEM SPECIFICATIONS

The specification for the recommended sounder configuration (Figure 9-1) follows. Figure 9-2 is a curve of S/N versus range for the sounder.

	Sounding Frequency (Mc)	Pole Length of Dipole (feet)	Antenna Matching Loss (db)	Radiated Power (watts)	Generated RF Power (watts)	Received Signal Power at Receiver Terminals Min (dbm)	Max (dbm)	Noise Power at Receiver Terminals (dbm) in 1 kc BW
Mars	1.0	60	10.5	20.0	224.0	-98.7	-73.2	-85.1
	2.0	60	3.4	16.0	35.0	-98.7	-73.2	-85.1
	5.0	60	1.0	12.3	15.5	-105.7	-79.9	-91.8
Venus	4.5	30	2.5	4.5	7.9	-105.7	-81.6	-92.1
	6.0	30	1.5	4.0	5.6	-107.7	-83.6	-94.1
	9.0	30	1.0	3.6	4.5	-111.2	-87.1	-97.6

Maximum sounding range: 40,000 km

Minimum sounding range: 8000 km

Receiver input dynamic range: 24.4 db

Transmission modulation: Angle modulation at 150 cps, with maximum phase deviation of $\pi/4$ radians pulsed at a 2-cps rate with a 50-percent duty cycle.

Sounding Duration: Three frequencies sequenced, with 8 seconds sounding time at each frequency.

Receiver: Superheterodyne, with one stage
                                 of tuned RF amplification.

                                 3.5-Mc IF, with bandwidth fixed
                                 at 1 kc by a crystal filter
                                 whose phase characteristic is
                                 linear with frequency to within
                                 3 degrees per 150 cps.

                                 Minimum of 10 db of limiting
                                 after crystal filter for -98 dbm
                                 signal in 1-kc bandwidth at
                                 receiver input.

                                 Phase-lock loop at IF, with min-
                                 imum information bandwidth of
                                 1 cps and two-sided noise band-
                                 width of 6.66 cps. Provides
                                 21.8 db carrier S/N improvement
                                 over IF S/N.

Data Measurement: Two 150-cps phase detectors in
                                 quadrature, each followed by
                                 "integrate and dump" filters with
                                 two-sided noise bandwidths of
                                 0.125 cps (8-second integration
                                 times).
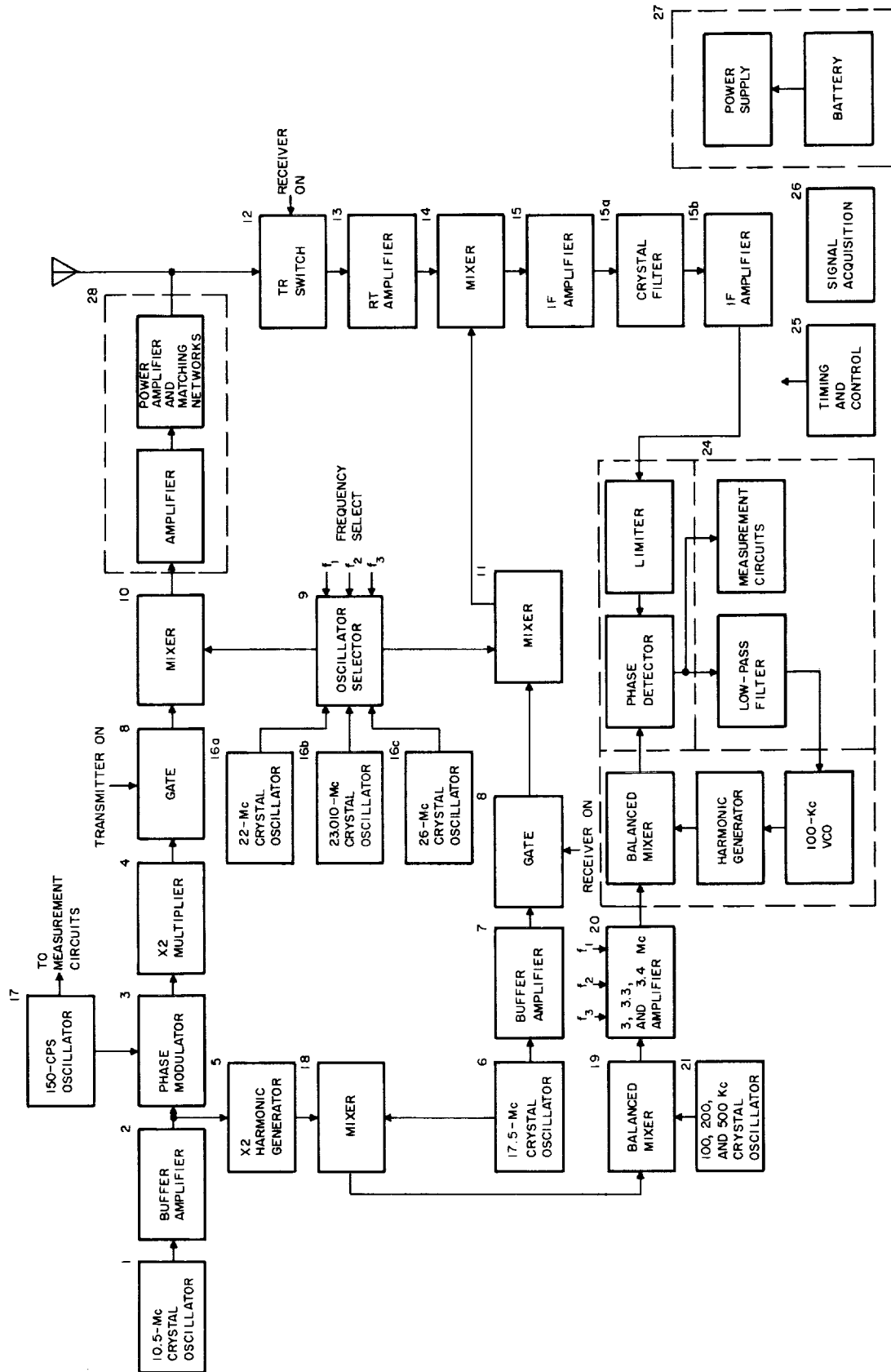
FIGURE 9-1. BLOCK DIAGRAM OF MARINER TOPSIDE SOUNDING EXPERIMENT FOR MARS

NO MODULATION
SPECULAR SIGNAL REFLECTION
$T_{EFF} = 500 \ (100/fmc)^{2.3}$
1-CPS THRESHOLD INFORMATION BANDWIDTH
60-FOOT DIPOLES FOR MARS
30-FOOT DIPOLES FOR VENUS

NOT INCLUDED:
DIPOLE DIRECTIVITY GAIN
FARADAY ROTATION LOSS
SCATTER AND NON-SPECULARITY LOSS
ABSORPTION LOSS
NOTE: S/N DURING MODULATION 1.4 db LESS

PHASE MEASUREMENT S/N (8-SECOND
INTEGRATION TIME) 11.7 db GREATER

VENUS

MARS

GENERATED RF POWERS:
224.0 WATTS AT 1.0 Mc ⎱
35.0 WATTS AT 2.0 Mc ⎰ MARS
15.5 WATTS AT 5.0 Mc

7.9 WATTS AT 4.5 Mc ⎱
5.6 WATTS AT 6.0 Mc ⎰ VENUS
4.5 WATTS AT 9.0 Mc

RANGE IN KILOMETERS X 10^3

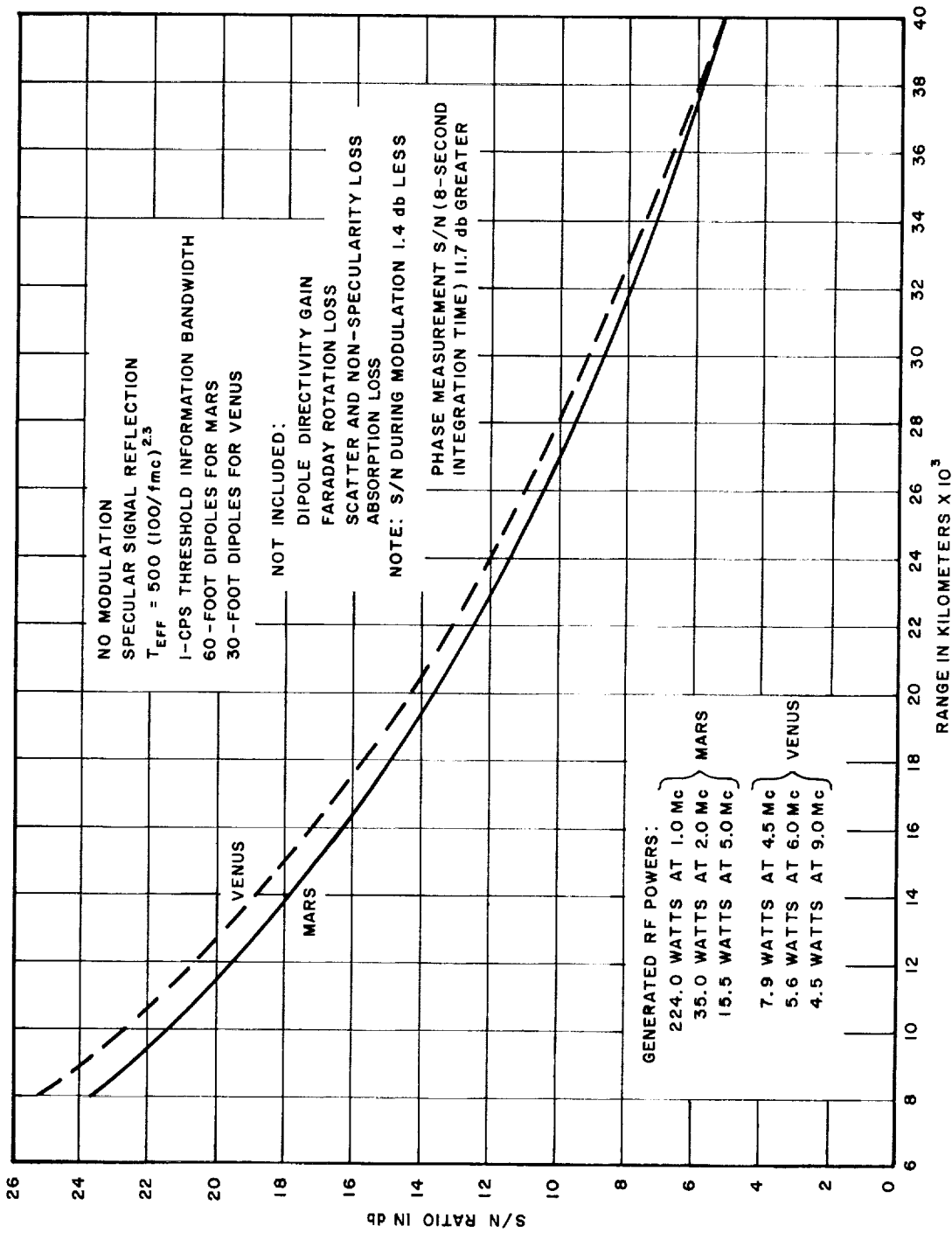S/N RATIO IN db

FIGURE 9-2. PHASE-LOCK LOOP S/N VS RANGE FOR PLANETARY
IONOSOUNDER

X.   IONOSOUNDER SYSTEM COMPONENTS

Those techniques discussed in the preceding sections that were considered critical were evaluated in the laboratory with a breadboard ionosounder. A two frequency sounder that contained most of the components described in this section was assembled and operated as predicted. The exceptions not included in the breadboard were:

1. Timing and control was limited to receiver and transmitter on-off control,

2. Matching networks and power amplifiers were not included,

3. Phase-lock loop did not contain the low-pass filter disconnect switch,

4. Signal acquisition was much simplified and involved the acquisition of system drift (no doppler simulation was used) with a VCO sweep of about 100 cps.

The following is a description of the recommended system components and their design approaches.

A.   RF SIGNAL GENERATION

The RF signal generation unit (Figure 10-1) is programmed to supply a phase-modulated signal to the transmitter every half second for a quarter of a second, and a local-oscillator signal (which is greater in frequency than the transmitter signal by an amount equal to the IF frequency) to the receiver during the remaining quarter of a second. This procedure continues for 8 seconds and is repeated sequentially for three different pairs of transmitter and LO frequencies.

1. SYSTEM OPERATION

The sounding frequencies are generated by mixing two crystal-controlled frequencies. A 10.5-Mc crystal-controlled oscillator is phase modulated with a 150-cps sine wave, and then doubled to 21.0 Mc. The modulated 21-Mc signal is then mixed with an output of one of the three crystal-controlled oscillators producing a difference frequency that is the sounding frequency.

The LO signals for the receiver mixer are also generated by mixing two crystal-controlled sources. The output of a 17.5-Mc crystal oscillator mixes with one of the outputs of the three crystal oscillators to produce the LO frequency that is higher than the signal being transmitted by an amount equal to the IF frequency (3.5 Mc).

All of the RF generation circuitry can be used for both the Mars and Venus flights, with the exception of the 22-Mc, 23-Mc, and 26-Mc oscillators and the LO mixer. It was found in breadboard tests that the same LO mixer could not be used for both flights. When the mixer filter's upper cutoff frequency was made high enough to pass the highest frequency for the Venus system, the outputs for the lower Mars frequencies were rich in harmonic content. This harmonic-rich LO caused large spurious responses in the receiver. These responses could have been filtered by the preselector, but the preselector would have become a great deal more complex.

2. INTERNAL FREQUENCY SELECTION

The choice of oscillator frequencies for the RF generation circuitry were based on the following:

1. Desirability of the internal frequencies to be separated in frequency by as much as possible from the output frequencies for ease of filtering.

2. Desirability of the oscillator frequencies to be higher than the sounding and LO frequencies, so that their harmonics will not impose restrictions on the output filtering.

3. Frequencies of the crystal oscillators should not be greater than 30 Mc, because crystals in this range are fragile.

The 22-Mc frequency that is referred to is a nominal value. Breadboard tests indicated that when the system was operating at 1 Mc (22-Mc oscillator in the circuit), leakage from the 23-Mc oscillator beating with the 22-Mc oscillator produced a 1-Mc leakage signal. This same phenomenon occurred when the system was operating with a sounding frequency of 2 Mc (23-Mc oscillator in the circuit). Leakage from the 22-Mc oscillator produced a 1-Mc signal whose second harmonic produced an interfering signal. To alleviate this problem, the frequency of the 22-Mc oscillator was increased by 2.5 kc, so that the leakage signal would be attenuated by the crystal filter in the receiver.

The 21-Mc signal in the transmitter signal circuitry is not generated directly, because the phase modulator that was used in the system was not linear for phase deviations up to the required ± 45 degrees. Because of this, a 10.5-Mc signal was phase modulated ± 22.5 degrees, and then doubled to produce a 21-Mc signal with a phase deviation of ± 45 degrees.

The phase modulator consists of a series resonant circuit where the capacitor is replaced by a pair of voltage-tuned varactors. The phase shift through this network is given by:

$$\theta = \tan^{-1}\left(\frac{\omega L - 1/\omega c}{R}\right) \tag{10-1}$$

where

ωL = inductive reactance of the series tuned circuit,

$1/\omega c$ = capacitive reactance of the two varactors in series,

R = sum of driving resistance and load resistance.

The voltage-capacitance relationship of an abrupt junction varactor can be given approximately by:

$$\frac{C}{C_o} = \left(\frac{V}{V_o}\right)^{-1/2} \tag{10-2}$$

where

    C = capacitance at voltage V,

    V = instantaneous voltage,

    C_o = capacitance at voltage V_o,

    V_o = DC bias on varactors.

Combining (10-1) and (10-2):

$$\theta = \tan^{-1}\left[\frac{\omega L - \dfrac{1}{\omega C_o (V/V_o)^{-1/2}}}{R}\right] \tag{10-3}$$

If the phase modulator is set up so that the quiescent capacitance C_o is made to resonate with the inductance at the incoming frequency, then:

$$\omega L = \frac{1}{\omega C_o} \tag{10-4}$$

Further, the quiescent Q can be given by:

$$Q_o = \frac{\omega L}{R} = \frac{1}{\omega C_o R} \tag{10-5}$$

Combining (10-3) and (10-5):

$$\theta = \tan^{-1} Q_o \left[1 - (V/V_o)^{-1/2}\right] \tag{10-6}$$

10-4

Similarly for a parallel tuned circuit:

$$\Theta = \tan^{-1} Q_o \left[1 - (V/V_o)^{-1/2} \right] \qquad (10\text{-}7)$$

Equations 10-6 and 10-7 are plotted in Figure 10-2, where it can be seen that for $Q_o = 1$ the series circuit is more linear than the parallel circuit. The curves also show that linearity improves with increased Q_o. However, large values of Q make the circuit sensitive to changes in the circuit parameters.

It is desirable that the phase-shift modulating voltage characteristic of the modulator be linear. If the circuit Q is assumed to be large, the circuit nonlinearity can be assumed to be due to the nonlinearity of the tangent characteristic. Examination of the characteristics of tangents shows that for a deviation of 45 degrees the maximum deviation from linearity is 17.2 percent. However, if a signal is modulated at 10.5 Mc by ± 22.5 degrees, then the maximum from linearity is only 3.9 percent. Two varactors are placed back-to-back in the circuit to improve the linearity with respect to the incoming 10.5 Mc. By using two varactors, calculations show that an incoming signal at 10.5 Mc of 1 volt rms will experience a peak departure from nonlinearity of 5 percent.

3.   GATING

The selection of transmitter and LO frequencies is performed by switching continuously operating oscillators into the system rather than turning the oscillators on. This was done because of the relatively long turn-on times for crystal oscillators (typically, 1 msec), and the possibility of frequency drift of the oscillators due to thermal warmup.

Gating was also used in place of filtering to eliminate leakage signals. The largest leakage problem in the breadboard was the rejection of 3.5 Mc wherever generated. Any 3.5-Mc signal that is generated and couples to the receiver must be attenuated below the receiver threshold. A possible mode of generation of 3.5 Mc is through 21 Mc leaking across the oscillator amplifier (Figure 10-1) to the LO mixer where it mixes with 17.5 Mc to produce 3.5 Mc. To eliminate this leakage path, the second harmonic generator, gate, and mixer in the transmitter signal line are gated off when the receiver is on.

A second path for leakage is through the power amplifier, and the antenna matching network to the RF amplifier. The leakage through this path is made negligible by turning the transmitter driver amplifier off during the receiving time.

The LO mixer (Figure 10-1) is turned off so that the 17.5-Mc signal does not modulate the transmitter signal. The receiver LO signal is also removed during transmit times.

It was found necessary to turn the first stage of the IF amplifier off, because of the transient characteristics of the crystal filter. When the transmitter is on and with no gating in the IF amplifier, some transmitted signal will leak through to the crystal filter. When the transmitter is turned off, this signal decays and extends into the receiver on-time. By turning the first stage of the IF amplifier off during the transmit time the problem was eliminated.

4. ALTERNATIVE METHOD OF RF FREQUENCY GENERATION

An alternative RF generation system that was breadboarded and tested is described in Appendix F. It has the advantage of requiring the frequency stability of the crystal oscillator to be only 1/11 as stable as the system in Fig-

10-6

ure 10-1. This system was breadboarded, tested, and found to have the following disadvantages:

1. The system required 8 transistors as compared with 4 transistors in the system in Figure 10-1, resulting in a larger volume, more weight, a greater power drain, and an increased hazard rate.

2. The output of the fractional-frequency multiplier in LO circuitry inherently had an output at 21 Mc as well as the desired 17.5-Mc output. The presence of a 21-Mc signal in the 17.5-Mc circuitry produced a component at 3.5 Mc that leaked into the receiver mixer. To reduce this signal below thermal noise, about 100 db of filtering was required.

3. A 3.5-Mc leakage signal was also produced by 21 Mc leaking back through the 21-Mc buffer amplifier to the 17.5-Mc buffer amplifier (Figure F-1).

For the preceding reasons and because the required stability for the double oscillator system of 3.8×10^{-6} can be obtained without an oven, the system shown in Figure 10-1 was chosen as the better system.

B. MATCHING NETWORKS

The matching network (Figure 10-3) has the following functions:

1. Converts the unbalanced output of the power amplifiers to balanced outputs for the antenna,

2. Reactively matches the antenna to the power amplifiers.

For the Mars flight (60-foot dipoles), matching inductors are used at 1 Mc and 2 Mc to form a series resonant circuit with the capacitive reactance of the antenna. At 5 Mc, the antenna appears inductive and capacitors are used for matching. Twin inductors and capacitors are placed on

the balanced side of the balun instead of single inductors or capacitors on the unbalanced side because: (1) the reactance (which is large for 1 Mc) can be shared by two inductors with half the inductance value, and (2) the power dissipated in the coil (158 watts in the case of 1 Mc) can be shared by two coils.

The band-reject filters are included so that the power amplifier in operation is not loaded down by the other amplifiers. The filters are designed so that the impedance at frequencies other than at the reject frequencies is negligible (typical insertion loss = 0.04 db).

The baluns in the matching network are ferrite toroidal transformers. The turns ratios are chosen so that the same supply voltage can be used for each frequency and the breakdown voltage of the transistors is not exceeded.

The insertion losses shown in Figure 7-1 were calculated for 60-foot and 30-foot dipoles and assumed matching coil Q's of 100 and a loss of 1 db for the baluns.

C.   POWER AMPLIFIERS

The power amplifiers consist of single transistor common-emitter amplifiers except for the 1-Mc amplifier for the Mars flight, which consists of two transistors in parallel in the common-emitter configuration. The transistors suggested (2N1900) for use have their collectors electrically connected to the case. The case will then be connected to the chassis to ensure a low thermal resistance.

D.   150-CPS GENERATION CIRCUITRY

The 150-cps generation elements (Figure 10-4) deliver a 150-cps sine wave to the phase modulator, and a pair of quadrature related square waves to the 150-cps phase detectors. The sine wave is generated by an RC oscillator.

The square-wave output is obtained by feeding one output of the oscillator to a flip-flop. Another output is fed through a two-section 90-degree RC phase shifting network to another flip-flop.

E.   RECEIVER

The receiver (Figure 10-5) is a single conversion superheterodyne design consisting of three TR switches, tuned RF amplifier, mixer, IF amplifier, and crystal filter. All of these except the tuned RF amplifier can be used for both the Mars and Venus flights. The RF amplifier must be unique for each flight, because the spurious responses in the Mars flight would fall into the band pass of the Venus flight. If these spurious responses were not filtered, additional cosmic noise would enter the receiver at these frequencies, and the sensitivity of the receiver would be degraded.

The noise figure of the receiver is relatively unimportant, because the expected level of cosmic noise power entering the receiver will be greater than thermal noise by amounts ranging from 49 db at 1 Mc to 36 db at 9 Mc.

The mixers (Figure 10-1) were designed with resistive input couplings, so that they could be operated for both the Mars and Venus flights without retuning the input circuitry. The transmitter mixer has a low-pass filter (f_{co} = 9 Mc) on its output, and as a result can be used for the Mars and Venus flights. The LO mixer has a three-pole network on its output with each pole tuned to a separate LO frequency, and thus must be tuned for each flight.

The receiver has an overall gain of 100 db, a bandwidth (which is determined by the crystal filter) of 1 kc, and a noise figure less than 10 db (not including the loss of the matching network). It has a rejection to all spurious signals of at least 25 db, and the combined

effect of all noise introduced by spurious responses affects the sensitivity by less than 1 db.

The TR switches consist of two diodes back-to-back, which are biased into their forward conduction regions (low attenuation) when the receiver is on, and into their nonconduction region (high attenuation) when the transmitter is on. Two diodes are used in a back-to-back configuration, because a peak RF voltage of 50 volts is expected across the TR switch. Thus, a single diode would require a breakdown voltage of 100 volts and a bias voltage of 50 volts to operate properly. Using the back-to-back configuration, a breakdown voltage of 50 volts can be tolerated with only a few volts of bias. The TR switch used in the breadboard had an attenuation of 3.5 db and provided 50 db of isolation at 1 Mc.

The placement of the crystal filter in the system is a compromise. If the filter is placed at the front of the amplifier chain, the wide-band noise that is generated after the filter might affect the system sensitivity. However, if the filter is on the output of the amplifier, the wide-band noise due to the earlier stages would saturate the amplifier reducing the signal level at the filter input. The crystal filter was put in the middle of the amplifier in the breadboard. The filter terminating impedances were padded with 750-ohm resistors to minimize changes in the filter characteristics due to changes in the impedances of the transistors. The overall filter loss including these padding resistors is 18 db.

F.   VCO LOOP FREQUENCY SYNTHESIZER

The VCO loop frequency synthesizer (Figure 10-6) provides signals to the phase-lock loop at 3.0, 3.3, or 3.4 Mc upon command. The signals are derived by mixing the second harmonic of the output of the 10.5-Mc crystal

oscillator with the output of the 17.5-Mc crystal oscillator, producing 3.5 Mc. The 3.5-Mc signal is then mixed with either 100 kc, 200 kc, or 500 kc, giving signals at frequencies of 3.0 Mc, 3.3 Mc, or 3.4 Mc. The 100-kc, 200-kc, and 500-kc signals are derived from a single crystal-controlled, 100-kc oscillator followed by a harmonic generator whose harmonic number output can be selected.

A 17.5-Mc tuned amplifier was included in the circuitry to prevent the 3.5 Mc that is generated in the 3.5-Mc mixer or the 21.0 Mc (which could beat with the 17.5 Mc at some other point producing 3.5 Mc) from reaching the local oscillator line. In the breadboard system, the 3.5-Mc leakage arising from this path was reduced to a level at least 10 db below thermal noise at the output of the IF amplifier. The 100-kc and 200-kc filters are single-tuned parallel circuits. The 500-kc filter is a double-tuned circuit. These circuits are all connected in parallel at the collector of the harmonic generator, with each circuit having a back-biased diode in series with it. When a particular harmonic is desired, the diode connected to the tuned circuit of the desired frequency is forward biased thus putting it into the system. In each of these circuits, the unwanted harmonics are suppressed by at least 20 db.

A balanced mixer is used in place of a conventional mixer to generate the 3.0-, 3.3-, and 3.4-Mc signals to suppress the input 3.5-Mc signal.

The output of the balanced mixer is fed to a three-pole Tchebycheff filter with buffer amplifiers on its input and output. The filter passes 3.0, 3.3, and 3.4 Mc and has a relative attenuation of 10.6 db for 3.5 Mc and 20 db for 3.6 Mc.

G. PHASE-LOCK LOOP

1. MARS SOUNDER

The phase-lock loop (Figure 10-7) design criteria is set by the system specifications and the optimization requirements (Appendix C). The threshold information bandwidth requirement of 1 cps yields a two-sided noise bandwidth of $\frac{3\pi}{\sqrt{2}}$ x 1 cps, or 6.66 cps. Arbitrary limiting of the maximum average phase offset to 1/6 radian at a maximum doppler shift of 25 cps would fix the open loop gain, G_T, at:

$$G_T = \frac{(25 \times 2\pi)\dfrac{\text{Radians}}{\text{second}}}{1/6 \text{ Radians}} = 300\pi \frac{\text{Radians/second}}{\text{Radian}}$$

The low-pass filter components are fixed by

$$t_1 = \frac{G_T}{B_o^2} = \frac{300\pi}{(2\pi)^2}$$

$$t_1 = \frac{300}{4\pi} = 23.8 \text{ seconds}$$

and

$$t_2 = \frac{\sqrt{2}}{B_o} = \frac{\sqrt{2}}{2\pi} \text{ if } \frac{t_2}{t_1} \ll 1$$

$$t_2 = 0.224 \text{ seconds}$$

$$t_1 = R_1 C$$

$$t_2 = R_2 C$$

Let C be 50 μf (a bi-polar tantalytic capacitor)

$$C = 5 \times 10^{-5} \text{ farads}$$

$$R_1 = \frac{23.8}{5 \times 10^{-5}} = 4.76 \times 10^5 \text{ ohms}$$

$$R_2 = \frac{0.224}{5 \times 10^{-5}} = 4.48 \times 10^3 \text{ ohms}$$

The receiver is turned on only during the 1/4 second intervals during which a reflected signal return may occur. Thus the phase detector has no input during the remaining 1/4 second. The low-pass filter has a time constant of 23.8 seconds and would discharge about 1 percent during the 1/4 second receiver off-time. This is undesirable with large doppler shifts and should be stopped by including an electronic switch that disconnects the low-pass filter as shown in Figure 8-1. Suitable switches with off impedances of many megohms and offset voltages less than 0.1 mv are available for this use.

The threshold IF S/N is -14.8 db, which represents a signal voltage component about 1/6 of that at high S/N. The open-loop gain is a direct function of the signal voltage component and would, therefore, increase from the threshold value by a factor of 6 at high S/N.

Phase lock is maintained with the changing doppler shifts that accompany a change in sounding frequency, by using the VCO harmonic selection method mentioned in Section IV-C(3). This harmonic selection has the effect of making the open-loop gain proportional to the harmonic used. Thus, in the case of the Mars sounder with sounding frequencies of 1, 2, and 5 Mc, the gain at 5 Mc would be

5 times the gain at 1 Mc. This is not desirable due to its effect of causing an increase in the loop noise bandwidth. Making the loop phase detector gain inversely proportional to the sounding frequency will maintain the threshold loop gain at the design value of 300π. This can best be done by varying the gain of the signal driver at the phase-detector input.

Keeping the open-loop gain independent of the sounding frequency would appear to cause an increase in the phase offset at the higher doppler shifts associated with higher sounding frequencies. However, the signal-acquisition procedure used will limit the phase-lock loop dynamic tracking requirement to ±25 cps.

The 100-kc loop VCO can reliably provide a sensitivity of 600 cps/volt linearly over a ±1 kc range, using 2 varactors as the frequency-controlling element. (This will produce a loading impedance on the control voltage that is kept in the high megohm range.) The frequency synthesis method mentioned in Section III-C(3) to accommodate the sounding frequency dependence of the doppler shift makes use of the 3.0-, 3.3-, and 3.4-Mc signals that are selectively generated, by mixing the proper harmonic of a 100-kc crystal oscillator with 3.5 Mc from the RF generation components (described in Section X-D). The appropriate signal is mixed with the first, second, and fifth harmonic of the 100-kc VCO in a balanced mixer (which minimizes post-mixing filtering), producing a sum frequency of 3.5 Mc plus the doppler shift. The 100-kc VCO frequency will exactly equal the 100-kc crystal oscillator frequency when the doppler shift is zero and will differ from it by the doppler shift divided by the ratio of the sounding frequency in use to the lowest sounding frequency. Note that this difference frequency (detected by the 100-kc phase detector

of Figure 10-7) provides a very good and useful indication of the doppler frequency, and thus the doppler velocity component between planet and spacecraft.

The phase detector gain at threshold (K_{mT}) must equal

$$\frac{\text{Threshold open-loop gain}}{\text{VCO sensitivity}} = \frac{300\pi \dfrac{\text{Radians/second}}{\text{Radian}}}{600 \times 2\pi \dfrac{\text{Radians/second}}{\text{volt}}}$$

$$K_{mT} = 1/4 \text{ volt/radian}$$

The maximum phase-detector gain at high S/N will be six times greater or 1.5 volts/radian. Reference to Figure C-1 of Appendix C shows that the 3-db bandwidth, ω_{3db}, will then be 7.8 B_o. Thus

$$\frac{\omega_m}{\omega_{3db}} = \frac{150}{7.8} = 19.2,$$

and the modulation will be shifted in phase by 4.5 degrees (Figure C-2), which is compatible with the accuracy of this system.

2. VENUS SOUNDER

Analysis of the Venus sounder phase-lock loop parameters follows the same line as that for the Mars sounder.

The Venus sounding frequencies are 4.5, 6, and 9 Mc. The same frequency synthesis techniques are usable, but with the desired 100-kc harmonics now being the third, fourth, and sixth that mix with 2.9, 3.1, and 3.2 Mc to provide the 3.5-Mc tracking signal.

The phase-detector gain at threshold will still be 1/4 volt/radian, if the 100-kc VCO sensitivity is decreased by 1/3 to 200 cps/volt. The phase-detector gain will then have to be controlled to $\frac{4.5}{6} \times 1/4 \frac{volt}{radian}$ at 6 Mc, and $\frac{4.5}{9} \times 1/4 \frac{volt}{radian}$ at 9-Mc sounding frequency to keep the open-loop gain constant.

H. SIGNAL ACQUISITION

The requirements for signal acquisition are the generation and control of the VCO sweep, and the sensing of phase lock.

The sweep requirements are that the 100-kc VCO be swept in steps that result in 25-cps variations in the 3.5-Mc phase detector input and at a sweep rate of 2 cps/sec. Figure 8-1 illustrates how this may be done.

At the start of the acquisition procedure, all counters and flip-flops will be reset. The leakage gates will be closed permitting acquisition of the drift, and the step-VCO timing pulses (one each 16 seconds) will be directed to the drift-compensating counter until drift is acquired. Each step of the counter will add an increment of voltage to the input of the phase-lock loop low-pass filter, so the filter output voltage will produce the 2-cps/sec sweep. The VCO frequency will be initially offset by one-half of the maximum expected drift, so that the counter is assured of being able to compensate for the drift. The quadrature phase detector and 1-cps filter will sense the phase-lock (zero beat) state and cause the Schmidt trigger to initiate the doppler acquisition procedure. This consists of removing the signal leakage path, turning on the sounder transmitter, and causing the doppler four-stage counter to control the sweep. Prior to the start of the doppler counter, it will

be preset to a value below the anticipated doppler shift and sweep up toward it. This will ensure the doppler acquisition, but requires a programming of predicted doppler shifts.

Acquisition of the doppler shift will signal the start of modulation and the end of the acquisition mode, and of any further counting. Loss of phase-lock for a predetermined interval will reinitiate the acquisition procedure.

I.   150-CPS PHASE DETECTORS AND INTEGRATORS

The sensitivity of the 3.5-Mc phase detector in the phase-lock loop at threshold has been specified as 1/4 volt/radian. The phase modulation is $\frac{\pi}{4}$ radians, so the threshold amplitude of the demodulated 150-cps output will be $\frac{\pi}{4} \times 1/4 = \frac{\pi}{16}$ volts, zero to peak. Paragraph E of Section V indicated the need for a 10-cps band-pass filter to raise the S/N of the 150-cps tone from the -17.6 db threshold S/N to -0.6 db S/N. A stage of amplification with a "twin-T" RC network providing negative feedback (and thus frequency selective gain) will satisfy this need and provide about 10 db of gain for signals within its pass band.

The filtered tone plus noise will then be phase detected in two transformerless 150-cps phase detectors (Figure 10-8) operating in quadrature. Each phase detector is followed by a 4-second time constant, RC low-pass filter that is "dumped" at the end of each 8-second integration period. The phase detectors will have outputs ranging from 0 to ± 4 volts at high S/N and 0 to ± 2.8 volts when the phase detector input S/N is at the minimum of -0.6 db.
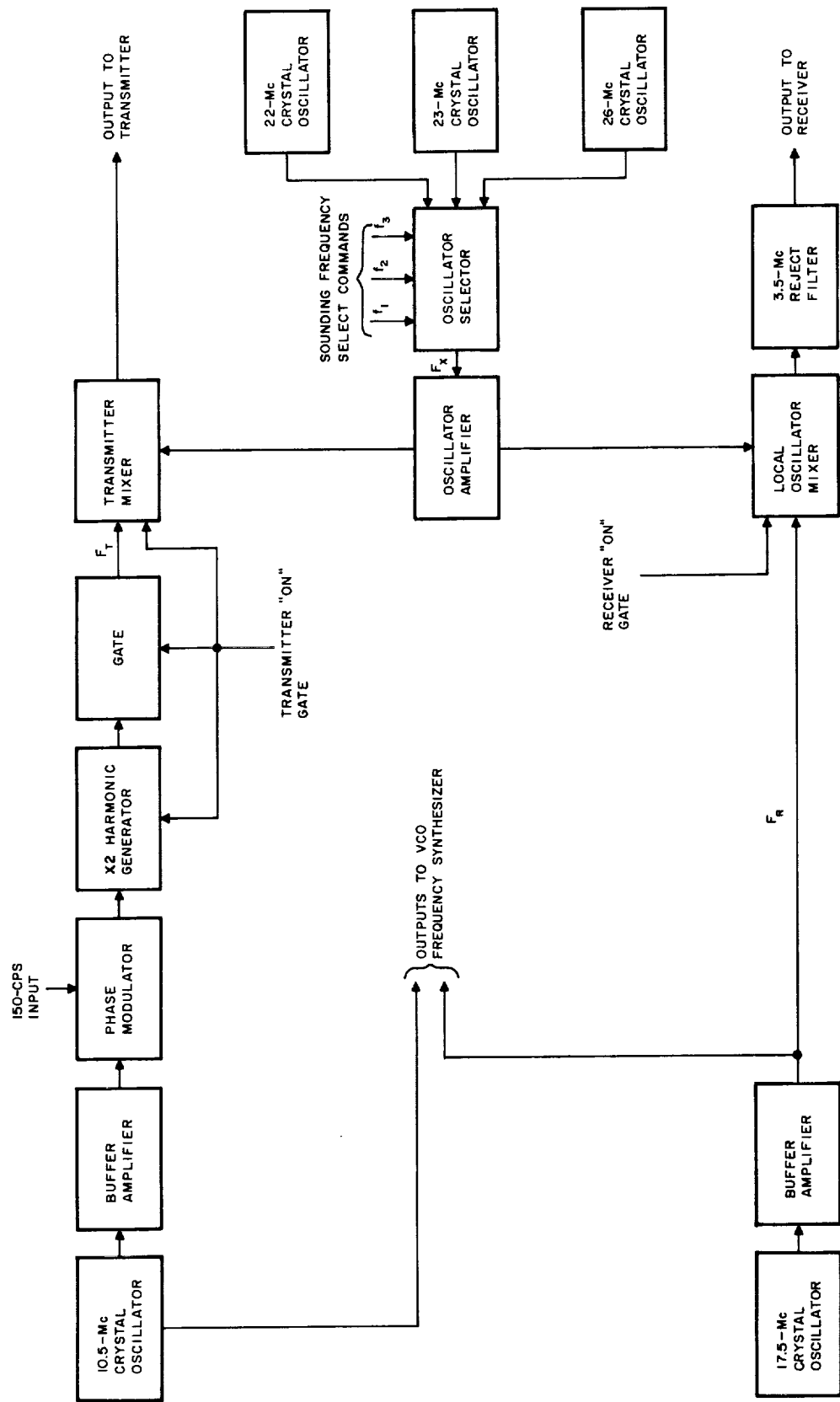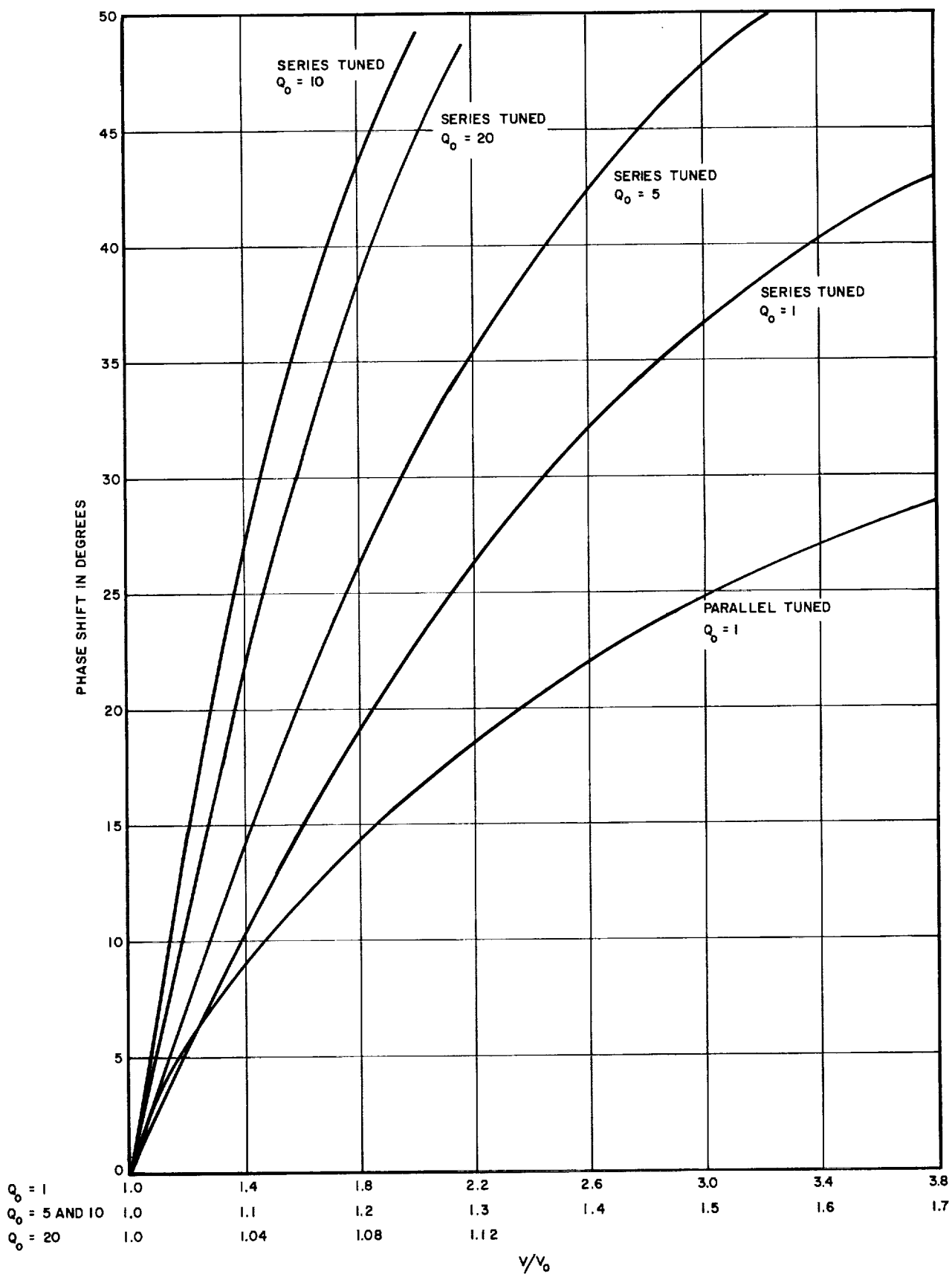
FIGURE 10-1. RF SIGNAL GENERATION UNIT

FIGURE 10-2.   PHASE-SHIFT CHARACTERISTICS OF SERIES AND
PARALLEL VARACTOR PHASE-SHIFT NETWORKS
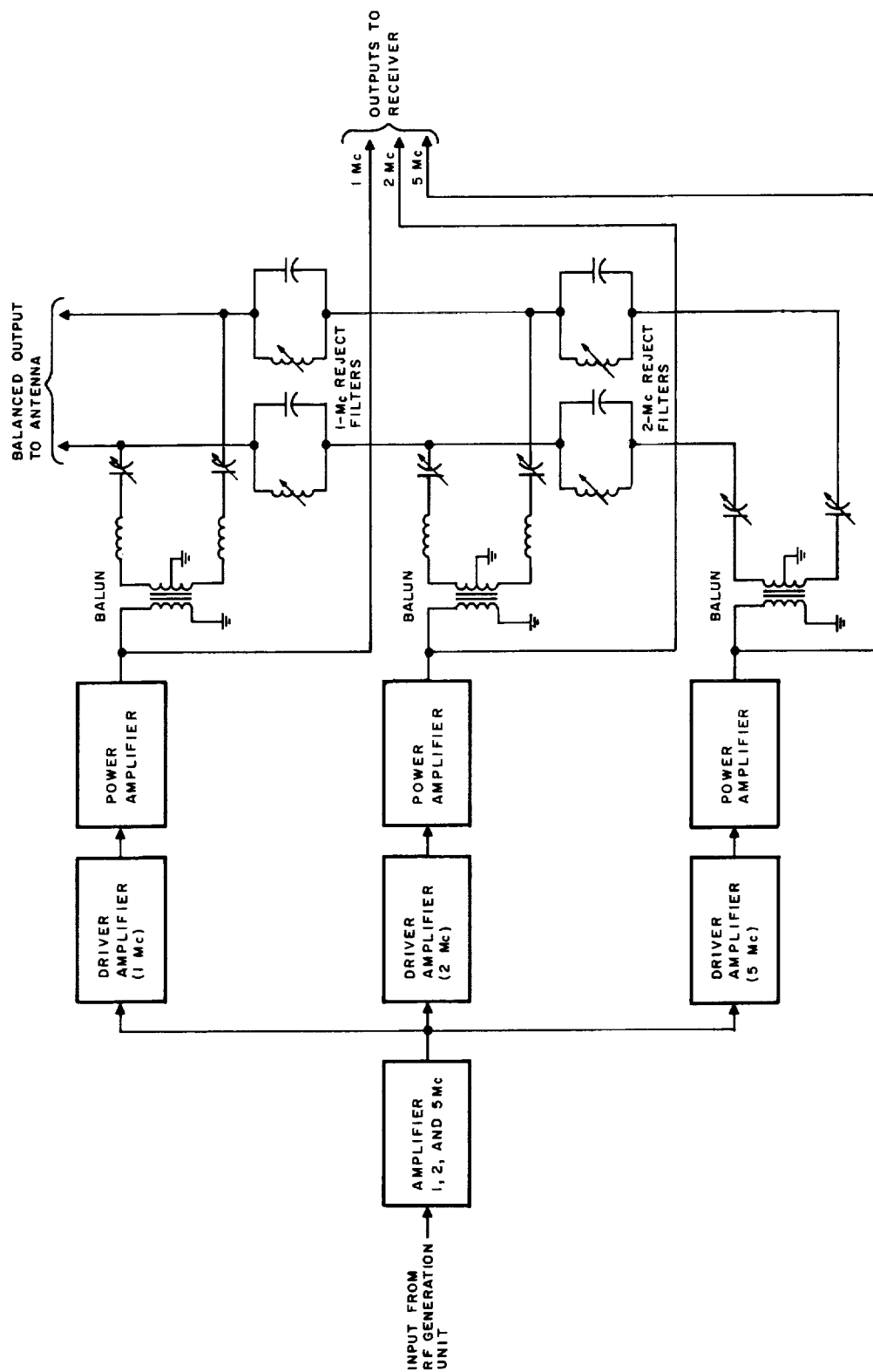
FIGURE 10-3. POWER AMPLIFIER AND MATCHING NETWORK (USING MARS FREQUENCIES)

OUTPUT TO
PHASE MODULATOR

150-CPS
OSCILLATOR → AMPLIFIER → 90-DEGREE
PHASE SHIFT → FLIP-FLOP → OUTPUT TO 150-CPS
PHASE DETECTOR NO. I
(QUADRATURE)

FLIP-FLOP → OUTPUT TO 150-CPS
PHASE DETECTOR NO. 2
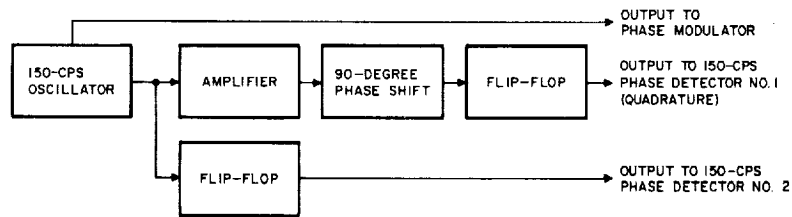
FIGURE 10-4.   150-CPS GENERATION ELEMENTS

INPUTS
FROM
MATCHING
NETWORK {
TR SWITCH
TR SWITCH
TR SWITCH

f_1 f_2 f_3
RECEIVER "ON" GATE

TUNED
RF AMPLIFIER → RECEIVER
MIXER → IF AMPLIFIER → CRYSTAL
FILTER → IF AMPLIFIER → TO PHASE
LOCK LOOP

LOCAL
OSCILLATOR
SIGNAL
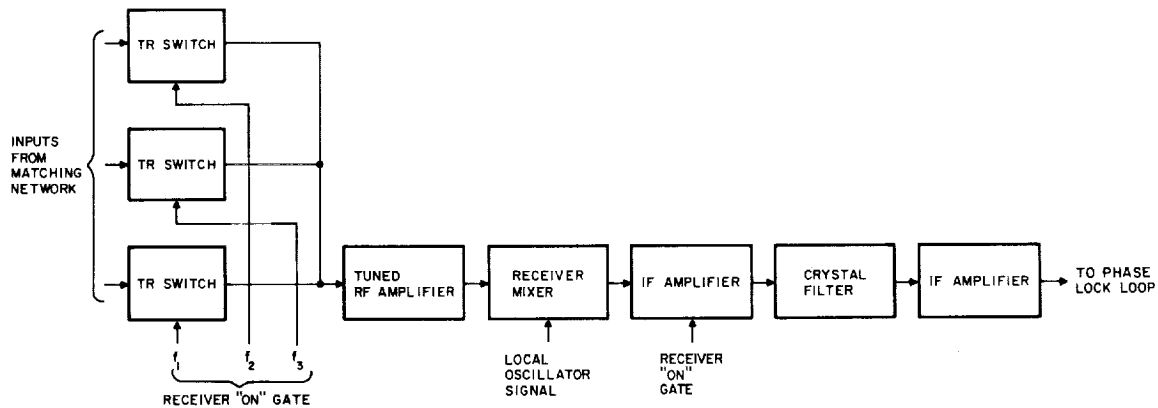
RECEIVER
"ON"
GATE

FIGURE 10-5.   RECEIVER BLOCK DIAGRAM

INPUT FROM
10.5-Mc
OSCILLATOR → X2
HARMONIC
GENERATOR

INPUT FROM
17.5-Mc
AMPLIFIER → 17.5-Mc
AMPLIFIER

3.5-Mc
MIXER → BALANCED
MIXER → BUFFER
AMPLIFIER → FILTER → BUFFER
AMPLIFIER → 30, 33, OR 34 MC
OUTPUT TO
VCO LOOP

X1, X2 OR X5
HARMONIC
GENERATOR

f_1
f_2
f_3 } HARMONIC
NUMBER
SELECTION

100-kc
CRYSTAL
OSCILLATOR
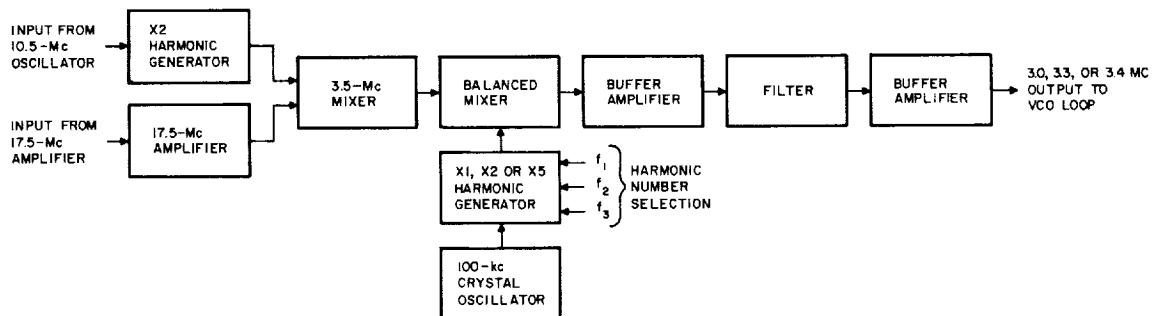
FIGURE 10-6.   BLOCK DIAGRAM OF VCO LOOP FREQUENCY
SYNTHESIZER

FIGURE 10-7. BLOCK DIAGRAM OF PHASE-LOCK LOOP AND RECEIVER
(MARS SOUNDER)

FIGURE 10-8.   MEASUREMENT COMPONENTS

XI. BREADBOARD PERFORMANCE

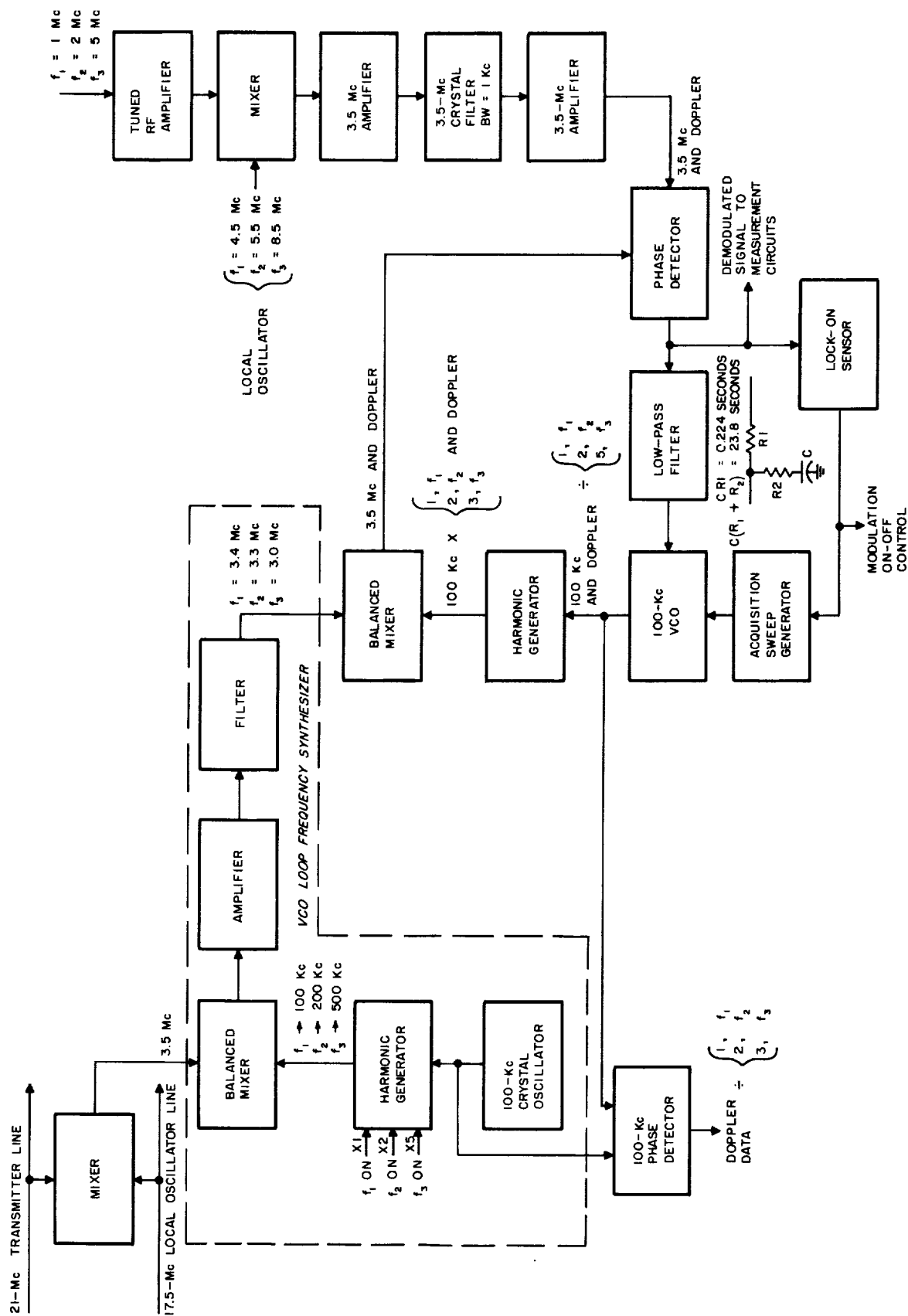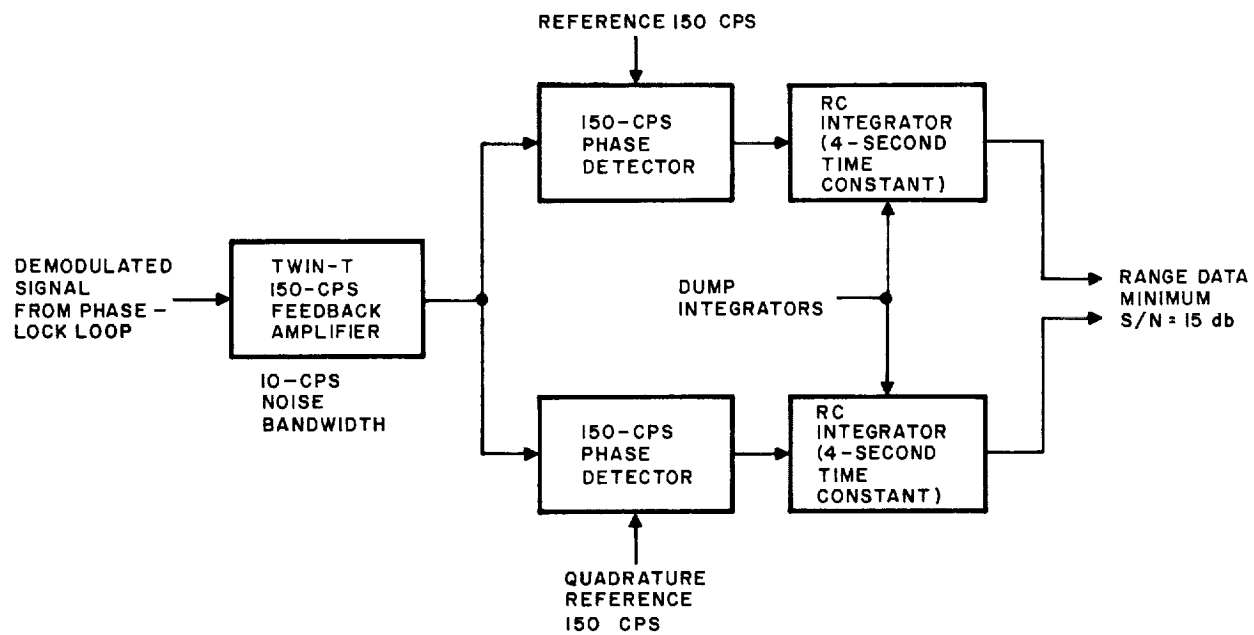A breadboard of the ionosounder components described in Section X was constructed to show the feasibility of the system design. The system parameters were then slightly modified, and the sounder used to demonstrate its function by performing bottom-side soundings of the ionosphere (Appendix G). The only significant problem in bringing the system into operation was the elimination of undesirable signals in the receiver that were originating in the RF generation components. These problems have been described in Section X.

The system was evaluated quantitatively under a simulated operating condition that allowed a known amount of leakage signal to appear in the receiver along with a measured amount of external noise. Figure 11-1 is a tracing of a recording made of the maximum output of one of the 150-cps phase detectors (zero phase difference between modulation and detected 150-cps tones) when the IF S/N ranges between -20 db and 0 db. The recordings agree well with the expected sounder performance and are an indication of the validity of the system design. (The phase detector output, which is in quadrature with the one shown, has an average output of zero for the phase difference measured.)

The variation in voltage outputs due to S/N changes does not affect the phase measurement as it is obtained from the ratio of the two phase detector outputs (Section IV-C).
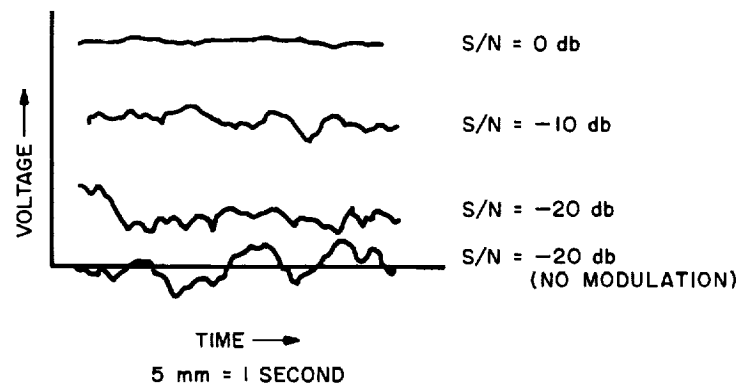
FIGURE 11-1.   RECORD OF MAXIMUM OUTPUT OF 150-CPS PHASE DETECTOR

XII. SYSTEM INTERFACES

The Timing and Control Section (VIII) mentions three control functions that are best handled through the system interface. These are antenna erection, power turn-on, and start and stop of sounding. There are three other functions that involve the system interface. These are:

1. Power for the sounder (exclusive of power amplifiers),

2. Provision for trickle charging the power amplifier battery to compensate for its self-discharge,

3. Facility for accommodating the two data-measurement outputs, as well as the information describing the sounded frequency and its time of occurrence.

The first function involves the ability to supply about 1.0 watt at about 12 volts.

The second calls for providing a constant current source of a few milliamperes for the life of the mission.

The third can, at this time, be specified only in terms of the measurement output signals due to the lack of knowledge about the spacecraft data-handling procedures.

The measurement data appears on two lines as voltage levels available for sampling at the end of each 8-second sounding interval. The voltage that appears at the end of this integration time will depend on the phase being measured and will have a maximum magnitude ranging between ± 2.8 volts at the minimum S/N and ± 4 volts at high S/N. The system resolution of 1/20 of the modulation period ($\pi/10$ radians) calls for a minimum voltage resolution of $1/5 \times 2.8$ volts or 0.56 volt for both polarities.

XIII. SYSTEM RELIABILITY

A. RELIABILITY ANALYSIS

Reliability estimates for the Mars and Venus experiments were obtained from the block diagram (Figure 9-1) and the estimated circuit components listed in Table 13-I. The reliability model used is based on the assumption that all components are considered to be serial, and the failure of any one part constitutes failure of the circuit.

Unless otherwise noted, hazard rates which were used are from MIL-HDBK-217 and are for high-quality parts used at about 25 percent of their rating, at about $25^{\circ}C$, and protected from vibration, shock, humidity, and other deleterious conditions. Where applicable, the Minuteman Parts hazard rates were also taken from MIL-HDBK-217 and they are based on an electrical stress of 0.2 at a temperature of $40^{\circ}C$.

It should be noted that the reliability of either experiment for the types of parts that are being considered for use is primarily a function of the coast time (3 to 12 months depending on whether or not a Mars or Venus probe is under consideration, and the launch window utilized) and not the use time (1 to 3 hours upon command). This is achieved by the use of sufficient derating and other protective measures which will ensure that the hazard rates of the parts are no greater during use than their hazard rates during shelf-life, which are the minimum hazard rates (used herein) that can be achieved.

Therefore, if the experiments survive the launch and coast periods, the probability of operating upon command is almost a certainty.

TABLE 13-I

ESTIMATED PARTS COMPLEMENT HAZARD RATES

Block Number on Figure 9-1	Estimated High Quality Parts Hazard Rate (fpmh)	Estimated Minuteman Hazard Rate (fpmh)
1	0.68	0.428
2	0.40	0.175
3	0.91	0.856
4	0.52	0.322
5	0.59	0.374
6	0.68	0.428
7	0.40	0.175
8	0.26	0.107
9	0.63	0.216
10	0.47	0.182
11	0.77	0.482
12	0.47	0.209
13	0.76	0.526
14	0.32	0.077
15	0.94	0.454
15a	0.80	0.800
15b	0.94	0.454
16a, b, c	0.276	1.593
17	0.65	0.129
18	0.72	0.477
19	0.26	0.053
20	0.78	0.528
21	1.27	0.766
22	2.10	0.714
23	2.71	1.189

TABLE 13-I (cont)

Block Number on Figure 9-1	Estimated High Quality Parts Hazard Rate (fpmh)	Estimated Minuteman Hazard Rate (fpmh)
24	2.20	0.289
25	6.71	0.680
26	1.44	0.198
27	3.98	2.634
28	4.98	4.554

The reliability (probability of survival) for both the Mars and Venus missions as a function of possible coast times are shown in Table 13-II. The basis for these computations are the parts complements of the Mars experiments (see Table 13-I). It was assumed that the Venus experiment would have approximately the same number of parts with differences existing only in frequency tuning and other applicable value changes. Reliability figures for both "high-quality" parts and Minuteman parts replacements as applicable (Table 13-I) are tabulated in Table 13-II for each coast time together with the percentage gains in reliability through substitution of Minuteman parts.

As can be seen from the results in Table 13-II, substitution of Minuteman parts can result in significant reliability gains for the Mars mission especially if the duration of the coast time approaches a year. Important parameters to be considered in using Minuteman parts are cost, availability, delivery schedule, and special handling.

TABLE 13-II

RELIABILITY ESTIMATES FOR MARS AND VENUS EXPERIMENTS

Coast Time (months)	3		4		5		8		9		10		11		12	
Part Types	High Qual.	M/Man.	High Qual.	M/Man.	High Qual.	M/Man.	High Qual.	M/Man.	High Qual.	M/Man.	High Qual.	M/Man.	High Qual.	M/Man.	High Qual.	M/Man.
Reliability	0.914	0.957	0.887	0.943	0.861	0.929	0.788	0.889	0.764	0.876	0.742	0.864	0.720	0.851	0.699	0.839
% Gain	4.7		6.3		7.9		12.8		14.7		16.4		18.2		20	

← Venus Mission → ← Mars Mission →

1.   PARTS AND MATERIALS APPLICATION

Organic materials may decompose and/or undergo
changes in their characteristics when exposed to high vacuum.
Materials containing plasticizer agents (that is, polyvinyl
chloride) that are volatile when exposed to vacuum should be
avoided.

High vacuum will also cause evaporation of some
metals and plastics. Large temperature gradients should be
avoided within the various electronic packages in the respec-
tive experiments, since such gradients, together with high
vacuum, will cause some metals and plastics to sublimate and
then recondense on cooler surfaces. Use of parts and materials
containing cadmium or zinc should be avoided.

Plastics that are reinforced with inorganic fillers
generally provide better radiation resistance than organic
materials. Also, the very poor radiation resistance of teflon
renders it nonusable for the Venus or Mars missions.

Germanium devices are capable of withstanding a
higher radiation environment than silicon devices; however,
the use of silicon is more desirable because of its superior
temperature characteristics. Transistors with a thin base
offer superior resistance to radiation; however, all semi-
conductors are more vulnerable to radiation than other compo-
nent parts. Since not all parameters are affected at the
same rate, careful circuit design will extend the tolerance
by allowing wider variations in susceptible parameters.
Overall protection by metal encasement (careful skin design)
will materially improve overall operation by accomplishing
some decrease in radiation intensity.

Wirewound resistors are relatively unaffected by a
radiation environment. Carbon and composition types can
exhibit resistance changes of 5 to 30 percent. Deposited-

film types are considerably more radiation-resistant than composition types.

Tantalum, paper-plastic, or mica types of capacitors should experience a minimum of difficulty if they are properly used (wide tolerances in capacitance and dissipation factor) and reasonably shielded by careful packaging.

No difficulty is anticipated in the use of inductors, transformers, batteries, and crystals if they are protected by careful skin design and packaging. However, it should be noted that further analysis and possible tests of the effects of radiation on these part types may become necessary when the specific radiation environments are better defined.

2. PREDICTION OF RELIABILITY

The mathematical model that was used to make the reliability prediction is based upon the results of extensive testing throughout the electronics industry and data gathered from operational equipments which have shown that the distribution of failure times of electronic parts and equipments can be expected to follow the exponential law:

The probability of failure during the interval (o, t) is $1 - e^{-\lambda t}$, where λ is the hazard rate, failure rate or mortality rate; λ represents the probability that, having survived to time t, the part fails in the interval $(t, t + \Delta t)$.

Under these conditions, the prediction of system reliability is reduced to the problem of determining the hazard rates of the individual component parts and then applying the familiar product rule:

$$R(t) = e^{-\lambda_s t}$$

where λ_s = the sum of all the component part hazard rates.

13-6

B.   SPACE ENVIRONMENT EFFECTS ON MARINER B EQUIPMENTS

The Mars and Venus missions of the Mariner B program have been analyzed in an attempt to determine whether electronics equipment subjected to the outer space environment for long periods of time would be adversely affected. For the purposes of this analysis the Mars mission is assumed to take place in the latter part of 1965 or in 1967 and to last about eight months. The Venus mission will take place in 1966 and have a duration of about four months. Two facets of the space environment present areas of possible danger to vehicle equipments: (1) high vacuum, and (2) radiation.

Vacuums as high as 10^{-14} torr may be met well away from the earth's atmosphere. Such a high vacuum will require special lubricants for movable mechanisms. Since it is not envisaged that lubrication will be important in AIL's phases of the Mariner B program, further discussion of possible lubrication methods is not developed here.

High vacuum can also cause evaporation of metals and insulation. If large temperature gradients exist within the vehicle together with a high vacuum, some metals and plastics can evaporate or sublimate and thereafter recondense on cooler surfaces. These surfaces may be electrically conducting such as in relays, etc. thus resulting in a conduction problem. Metals such as zinc and cadmium should be avoided. Most other metals including aluminum, germanium, and silicon will not sublime appreciable at typical space vehicle temperatures.

Little information is available on the changing characteristics and decomposition of organic materials in vacuum, but preliminary data indicate that such polymers as nylon, sulphide, nitrate cellulose, oxidized cellulose, methyl acrylate, esters, epoxies, urethane, vinyl butyral, vinyl chloride, linseed oil, and neoprene may possibly be troublesome. Oils, greases, and plastics and elastomers which contain

plasticizer agents volatile in vacuum should also be avoided (for example, polyvinyl chloride).

The condensation problem can be reduced appreciably by permitting only small thermal gradients throughout the electronic areas. Note should be taken, however, that with elastomers containing volatile plasticizer agents, decomposition and condensation may not be the major problem. These materials often become brittle and crack with the loss of the plasticizer and therefore become unsuitable for use as insulation.

The radiation environment to which the Mars and Venus probes will be subjected consists of (1) solar electromagnetic radiation, (2) galactic cosmic radiation, and (3) solar corpuscular radiation. The first mentioned should not cause any problem to internally mounted equipments since the skin of the vehicle will provide adequate protection. Galactic cosmic radiation should not be damaging either because of the extremely small fluxes involved. Corpuscular radiation, however, may have some deleterious effects upon internal electronic equipments.

Because of the difficulty in describing the transient effects of radiation on entire circuitry, the area of transient damage is not discussed here. This should be an area for separate investigation.

Permanent damage effects are dependent upon the frequency of occurrence, spectra, and intensity of solar flares. There has been a large variation in the published data describing these parameters. The duration of a solar flare may range from minutes up to several days with associated particle energies of a few Mev up to several Bev. Total integrated intensities have approached a maximum of 10^{10} protons/cm^2 with energies greater than 10 Mev (sufficient energy for penetration of a 30-mil aluminum satellite skin).

It is estimated from the eleven-year solar cycle and the proposed times for the Venus and Mars flights, that the Venus flight (1966) will encounter a maximum of three intense solar flares and the Mars flight (1967) a maximum of six. From this estimate and the maximum proton flux per flare, the maximum integrated flux with energy greater than 10 Mev which could be encountered in each mission is:

$$\text{Venus flight} - 3 \times 10^{10} \text{ protons/cm}^2$$
$$\text{Mars flight } - 6 \times 10^{10} \text{ protons/cm}^2$$

As a guideline for predicting possible electronic equipment damage in the two flights, the thresholds for radiation damage for various electronic components are presented in Table 13-III. The lowest level of integrated flux which has produced any noticeable change in a component parameter in any radiation experiment has been used as the threshold. It should be mentioned that this level may not be typical for all components in each class since great variations in radiation level sensitivity have been found between components. Manufacturer, method of fabrication, and the presence of impurities have all been shown to affect radiation damage levels.

In cases where no experimental data on proton damage were available, fast neutron irradiation data were used. It can be assumed in this analysis of permanent damage effects that fast neutron damage and high energy proton damage are equivalent.

It is emphasized that the levels of Table 13-III are only guidelines to possible damage; there is a great lack of data concerning damage dependence on radiation intensity, radiation damage in high vacuum, and the respective effects of various types of corpuscular radiation.

TABLE 13-III
THRESHOLDS FOR RADIATION DAMAGE

Component	Threshold for Permanent Damage (particles/cm^2)	Type of Damage
Silicon transistors		
Thick base	10^{10}	Changes in gain, collector, and leakage currents
Thin base	10^{12}	Changes in gain, collector, and leakage currents
Germanium transistors		
Thick base	10^{11}	Changes in gain, collector, and leakage currents
Thin base	10^{13}	Changes in gain, collector, and leakage currents
Silicon diodes	10^{11} to 10^{12}	Increase in forward voltage drop, changes in reverse and forward current characteristics
Germanium diodes	10^{13}	Increase in forward voltage drop, changes in reverse and forward current characteristics
Resistors	10^{15}	Decrease in resistance
Potentiometers	10^{14}	Failure
Capacitors	10^{12}	Change in capacitance and dissipation factor
Electron tubes	10^{12}	Cracks in glass, metal seals, failure
Quartz crystals	10^{15}	Frequency changes
Flashlight dry cells	10^{16}	Some deterioration
Solar cells	10^{9}	Degradation of power output

In addition to the preceding components, certain
materials are sensitive to irradiation and should be avoided
if possible. Teflon and nylon are specific examples of
materials that are appreciably altered at low radiation levels
(10^{13} protons/cm^2).

It can be seen that for the missions under consider-
ation, permanent radiation damage does not appear to be a major
problem. Although the analysis indicates that the thresholds
for damage are approached for the semiconductor components,
this result is based upon many assumptions in areas where
little data are presently available--for example, the effects
of secondaries, radiation effects in high vacuum, flare
occurrence, flare type prediction, slowing down of particles
in skin and structural shielding, and overall circuitry
effects. In developing each assumption a conservative
approach has been taken, that is, any possible damage occur-
rence has been magnified. Therefore, it is most probable
that the true radiation environment will be greatly below
the semiconductor threshold for permanent damage.

It is recommended that for the greatest reliability
more radiation resistant components and materials be used
when possible in the final equipment design. Certain plastics
should be avoided, and the spacecraft thermal design should be
such so as to minimize any large temperature gradients across
the electronics compartment. The probability of radiation
induced transient effects affecting overall system performance
at a crucial moment should also be evaluated in the light of
additional analyses.

XIV. SYSTEM SIZE, WEIGHT, AND POWER REQUIREMENTS

The following values are based on using conventional point-to-point wiring techniques.

	Weight (pounds)	Volume (cubic inches)	Power (watts)
Ionosounder Electronics excluding Transmitter	12	175	1
Transmitter with heat sinks	3	30	(separate battery)
Dipole Antennas (60 foot)	5	140	-
Antenna Matching Networks	3	30	-
Battery	2.5	30	-
Total	25.5	405	1

XV. RECOMMENDATIONS

The planetary ionosounder has been designed to accommodate the environment expected for its operation. It has been tested in the laboratory and performs as expected. Laboratory operation did not, however, fully simulate the spacecraft operating environment. The characteristics of doppler shift and the true ionospheric reflections are ideally simulated only by actual topside sounding. Furthermore, the constructed breadboard did not contain all components needed for a complete sounder, and those that were built were designed to provide the necessary technique verifications with quick solutions of the basic component requirements.

It is, therefore, felt that future efforts toward the development of a Planetary Ionosounder should be directed toward the development and flight testing of a well-engineered model embodying the techniques and components recommended in this study. Flight testing would be undertaken in a rocket-test sounding the earth's ionosphere, and would provide system performance data under conditions closely approximating the environment of the planetary soundings.

XVI. REFERENCES AND BIBLIOGRAPHY

1. L. Jaffe and E. Rechtin, "Design and Performance of Phase-Lock Loops Capable of Near Optimum Performance Over a Wide Range of Input Signal and Noise Levels," Trans IRE, IT-1, p 66-76, March 1955.

2. B. D. Martin, "Threshold Improvement in an FM Sub-carrier System," Trans IRE, SET-6, p 25-33, March 1960. (Comment by J. J. Spilker appears in SET-7, p 55, June 1961.)

3. W. B. Davenport, Jr., "Signal-to-Noise Ratios in Band-Pass Limiters," Journal of Applied Physics, Vol 24, p 720-727, June 1963.

4. R. L. Choate, "Analysis of a Phase-Modulation Communications System," Trans IRE, CS-8, p 221-227, December 1960.

5. C. E. Gilchriest, "Application of the Phase-Locked Loop to Telemetry as a Discriminator or Tracking Filter, Trans IRE, TRC-4, p 20-35, June 1958.

6. W. J. Gruen, "Theory of AFC Synchronization," Proc IRE, Vol 41, p 1043-1048, August 1953. (Correction to paper appears in Vol 41, p 1171, September 1953.)

7. S. G. Margolis, "The Response of a Phase-Locked Loop to a Sinusoid Plus Noise," Trans IRE, IT, p 136-142, June 1957.

8. A. J. Viterbi, "Acquisition and Tracking Behavior of Phase-Locked Loops," Proc Symposium on Active Networks and Feedback Systems, Polytechnic Institute of Brooklyn, New York, April 1960.

9. B. D. Martin, "The Pioneer IV Lunar Probe: A Minimum-Power FM/PM System Design," Technical Report No. 32-215, Jet Propulsion Laboratory, 15 March 1962.

10. W. B. Davenport, Jr. and J. Root, "Random Signals and Noise," McGraw-Hill Book Co., New York, p 359, 1958.

APPENDIX A
PROPAGATION AND SIGNAL TO NOISE CONSIDERATIONS
IN IONOSPHERIC TOPSIDE SOUNDING

1. ## CHARACTERISTICS OF SIGNAL RETURNS

    a. ## REFLECTION

    Since normal reflection from the ionosphere may
be approximately represented by specular reflection from an
equivalent conductive surface at a depth fixed by the refrac-
tive index, computation will be based upon the assumption of
specularity. Non-specularity will be considered separately.

    When the curvature of the reflecting layer is suf-
ficiently small, the power-spreading loss associated with
reflection and return of the signal may be obtained by com-
puting the one-way power loss to an image-point at twice the
range.

    Since the planetary ionospheres have curvature, a
correction factor must be applied to account for the shrink-
ing of the Fresnel region from that of a flat reflector (that
is, defocusing). Figure A-1 shows the Fresnel regions for
planar and curved ionospheres for the two planets. Maximum
and minimum ranges and frequencies are shown. Figure A-2
shows the defocusing loss with respect to reflection from a
planar surface. The loss may be written:

$$L = \left[\frac{R_p}{R_p + d} \right]^2$$

as a power ratio where R_p is the radius of curvature of the
convex surface and d is the distance.

Equatorial bulge, in the event of a significant magnetic field, results in about ±2 db variation in the loss factor when the bulge is comparable to that of the earth's ionosphere.

b. ABSORPTION

Approximate absorption computations have been made for a Chapman ionization profile and rather extreme conditions. The calculations are not shown, since they only indicate that absorption is not an important factor, being less than 1 db round-trip even at 98 percent of the critical frequency. An estimate of the effect of electron-ion collisions was included.

c. FARADAY ROTATION

When long pulses of phase-modulated signal are transmitted, the two magneto-ionic components of the reflected signal will almost completely overlap, resulting in a Faraday polarization rotation. Because many rotations are involved at these frequencies, the polarization of the received wave may be regarded as random for any given time. The temporal behavior should follow a fading in and out pattern as the signal polarization aligns and disaligns itself with the receiver dipole orientation. Both observer motion and ionospheric motion should cause rotation changes. The cosmic noise is also randomly polarized, so that the signal and noise polarization losses will tend on the average not to affect the receiver S/N.

d. ANTENNA GAIN

Since external noise may be regarded as the dominant factor, receiving antenna efficiency is of no consequence, and directivity gain is sufficient to determine signal-to-noise improvement due to the antenna. Transmitting inefficiencies must be accounted for in obtaining actual radiated power.

For the range of frequencies used, and the antenna lengths of 30 feet and 60 feet for Venus and Mars, respectively, the dipole directivity gain varies from 3.6 to 4.4 db round-trip for optimum orientation. However, isotropic antenna gains will be used in system computations because of uncertainties in antenna orientation.

e.   SIGNAL-TO-NOISE RATIO REQUIREMENTS

A working signal-to-noise ratio will be obtained for the measurement and phase-locked loop (coherent detection) channels. The probability density of the phase, $P(\phi)$, of a sinusoid plus narrow-band noise for large signal-to-noise voltage ratio, x, is (from reference 10).

$$P(\phi) = \frac{1}{\sqrt{2\pi}\left[\frac{1}{\sqrt{2}\ x}\right]} e^{-\frac{\phi^2}{2\left[\frac{1}{\sqrt{2}\ x}\right]^2}}$$

which is Gaussian with σ of $\frac{1}{\sqrt{2}\ x}$.

If an accuracy of 50 km (corresponding to $\pi/10$ radians at the 150-cps modulation rate) is desired, with 95-percent assurance of falling within the 50-km zone, then the zone must be 3.92 σ's wide or x = 8.85, which is +19 db. For a zone of ±50 km, we require only +13 db.

After detection, the video S/N ratio will be given as the equivalent working S/N ratio providing phase accuracies in accord with the Gaussian distribution previously given. This may be obtained either by scaling the IF S/N ratio by the ratio of IF to two-sided video bandwidth, or the ratio of video integration time to IF impulse response time. This S/N ratio is also that used in determining phase-locked loop stability, where at least +4 db S/N ratio is required for initial lock-on.

2. REFLECTED SIGNAL-PATH ATTENUATION

The received signal power density from a large flat specular reflector lying in a plane normal to the propagation path at a distance d meters is p for an isotropic antenna with transmitted power P_T watts.

$$p = \frac{P_T}{4\pi(2d)^2} \text{ watts/m}^2$$

The effective area of an isotropic antenna is $\frac{\tau^2}{4\pi}$ where τ is wavelength of signal. Then the received signal power is P_R

$$P_R = \frac{P_T}{4\pi(2d)^2} \times \frac{\tau^2}{4\pi}$$

$$P_R = P_T \frac{\tau^2}{6.34 \times 10^2 d^2}$$

and $\tau = \frac{3 \times 10^2}{f_{mc}}$, f_{mc} = sounding frequency in Mc

Then:

$$P_R = P_T \frac{1}{7.05 \times 10^{-3} d^2 f_{mc}^2}$$

Substituting a curved surface with radius of curvature R_p causes an additional loss due to defocusing. This loss factor is $\left[\dfrac{R_p}{R_p + d}\right]^2$ and is plotted for Mars and Venus on Figure A-2 of this appendix.

A-4

3. COSMIC NOISE

The available thermal noise due to a source at temp T_{eff} is $KT_{eff}B$, where k is Boltzmann's constant and B is the bandwidth of the noise power.

The cosmic noise temperature has been found empirically to be $T_{eff} \cong 500 \frac{100}{(f_{mc})}^{2.3}$. Thus, in a 1-cps bandwidth, the cosmic noise power P_n is

$$P_n = 1.38 \times 10^{-20} \times 500 \frac{100}{(f_{mc})}^{2.3}$$

$$P_n = 2.76 \times 10^{-10}(f_{mc})^{2.3} \text{ watts in 1-kc bandwidth}$$

4. RECEIVED SIGNAL TO NOISE

The S/N per cycle of bandwidth available at an antenna's terminals is P_R/P_n.

$$\frac{P_R}{P_n} = P_T \frac{1}{7.05 \times 10^{-3}d^2(f_{mc})^2} \times \frac{1}{2.76 \times 10^{-10}(f_{mc})^{-2.3}} \times \text{defocusing loss}$$

$$\frac{P_R}{P_n} = P_T \frac{1}{1.945 \times 10^{-12}} \times \frac{f_{mc}^{0.3}}{d^2} \times \text{defocusing loss per cycle}$$
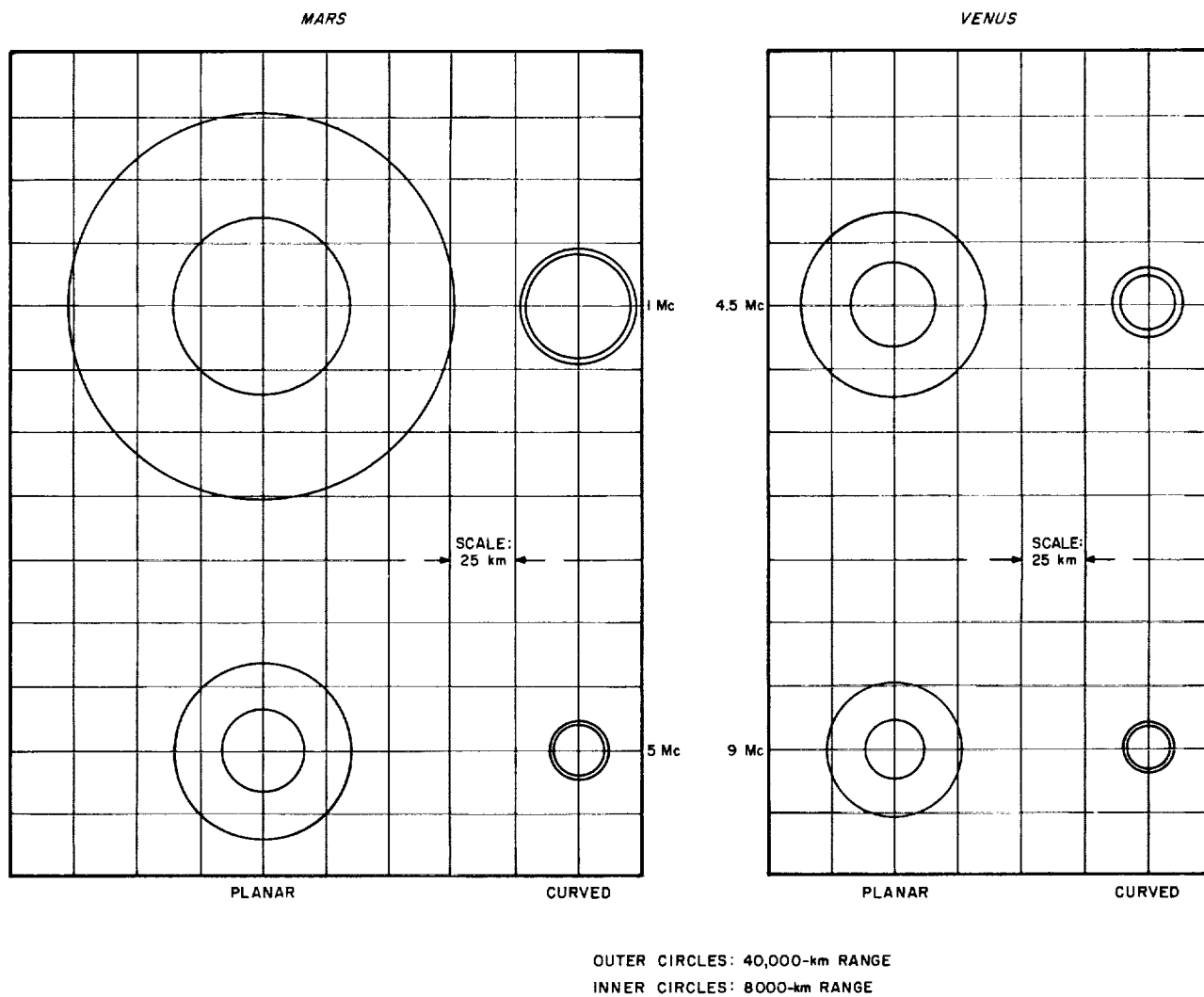
of bandwidth.

MARS   VENUS

1 Mc   4.5 Mc

SCALE: 25 km   SCALE: 25 km

5 Mc   9 Mc

PLANAR   CURVED   PLANAR   CURVED

OUTER CIRCLES: 40,000-km RANGE
INNER CIRCLES: 8000-km RANGE
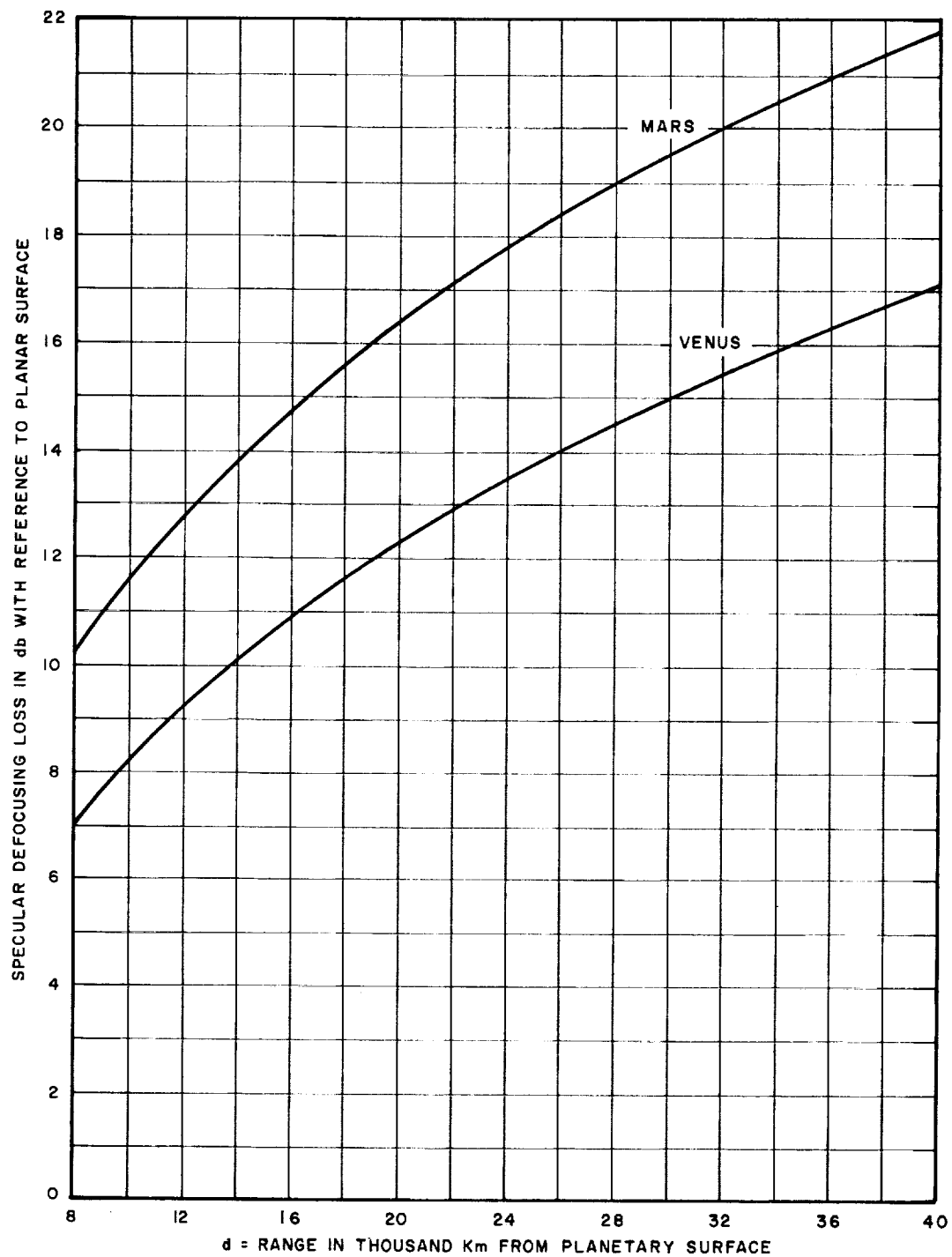
FIGURE A-1. FRESNEL REGIONS

FIGURE A-2. DEFOCUSING LOSS FACTOR

APPENDIX B
SIGNAL VARIATIONS DUE TO SPACECRAFT MOVEMENT

1. CARRIER FREQUENCY DOPPLER SHIFT

Referring to Figure B-1, the doppler velocity component relative to the planet is

$$V_D = V \sin \theta$$

$$= V \frac{Vt}{\sqrt{(Vt)^2 + d^2}}$$

$$= \frac{V}{\sqrt{1 + \left(\frac{d}{Vt}\right)^2}}$$

The doppler frequency shift is

$$f_d = -2f_c \frac{V_D}{C}$$

where

f_c = sounding frequency,
C = velocity of propagation;

and

$$f_d = -\frac{2f_c V}{C \sqrt{1 + \left(\frac{d}{Vt}\right)^2}}$$

The maximum doppler shift for any f_c will occur for d/t minimum at the maximum sounding range of 40,000 km where d = 30,000 km and Vt = 30,800 km. Then $f_d = -f_c \times 24 \times 10^{-6}$ cps.

The rate of doppler frequency shift is found by taking the time derivative of f_d.

$$\frac{\delta f_d}{dt} = \frac{-2f_c V}{C} \left[\frac{(\frac{d}{V})^2}{\left[t^2 + (\frac{d}{V})^2 \right]^{3/2}} \right]$$

This function is maximum for minimum d where d = 11,000 km and t = 0. Then:

$$\frac{\delta(f_d)}{dt} = 1.51 \times 10^{-8} \times f_c \text{ cps}$$

which equals 0.136 cps at $f_c = 9$ Mc.

2. MODULATION PHASE VARIATION (MEASUREMENT ERROR DUE TO SPACECRAFT MOVEMENT DURING TIME OF MAKING MEASUREMENT)

The round trip propagation time = τ.

$$\tau = \frac{\left[\sqrt{(Vt)^2 + d^2} - R \right]^2}{C}$$

Where symbols are the same as in paragraph 1, let

$$\tau_o = \frac{\left[\sqrt{(Vt_o)^2 + d^2} - R \right]^2}{C}$$

B-2

so that

$$\tau - \tau_o = \frac{2}{C}\left[\sqrt{(Vt)^2 + d^2} - \sqrt{(Vt_o)^2 + d^2}\right]$$

then let $t = t_o + \Delta t$:

$$\tau - \tau_o = \frac{2}{C}\sqrt{V^2 t_o^2 + d^2}\left[\sqrt{1 + \frac{V^2\Delta t^2 + 2V^2 t_o\Delta t}{V^2 t_o^2 + d^2}} - 1\right]$$

If

$$\frac{V^2\Delta t^2 + 2V^2 t_o\Delta t}{V^2 t_o^2 + d^2} \ll 1$$

then

$$\tau - \tau_o = \frac{2}{C}\sqrt{V^2 t_o^2 + d^2}\left[1 + \frac{V^2\Delta t^2 + 2V^2 t_o\Delta t}{2(V^2 t_o^2 + d^2)} - 1\right]$$

$$= \frac{1}{C\sqrt{V^2 t_o^2 + d^2}} \times \left(V^2\Delta t^2 + 2V^2 t_o\Delta t\right)$$

If T = modulation period, then

$\Delta\emptyset(t)$ = modulation phase variation during time interval Δt

$$= \frac{\tau - \tau_o}{T} \times 2\pi$$

$$= \frac{2\pi V^2}{CT\sqrt{V^2 t_o^2 + d^2}}\left(\Delta t^2 + 2t_o\Delta t\right)$$

The average value of the phase during a time interval Δt_o is $\overline{\phi(t)}$, which is the value obtained after integration of the modulation phase detector output for a time interval Δt_o.

$$\overline{\phi(t)} = \frac{1}{\Delta t_o} \int_0^{\Delta t_o} \phi(t)d\Delta t + \phi(t_o)$$

$$= \frac{2\pi V^2}{CT\Delta t_o} \sqrt{V^2 t_o^2 + d^2} \int_0^{\Delta t_o} (\Delta t^2 + 2t_o\Delta t)d\Delta t + \phi(t_o)$$

$$\int_0^{\Delta t_o} (\Delta t^2 + 2t_o\Delta t)d\Delta t = \left| \frac{\Delta t^3}{3} + t_o\Delta t^2 \right|_0^{\Delta t_o}$$

$$= \frac{\Delta t_o^3}{3} + t_o\Delta t_o^2$$

Then

$$\overline{\phi(t)} = \frac{2\pi V^2}{CT\Delta t_o \sqrt{V^2 t_o^2 + d^2}} \left(\frac{\Delta t_o^3}{3} + t_o\Delta t_o^2 \right) + \phi(t_o)$$

$$\overline{\Delta\phi(t)} = \frac{2\pi V^2}{CT\sqrt{V^2 t_o^2 + d^2}} \left(\frac{\Delta t_o^2}{3} + t_o\Delta t_o \right)$$

It is of interest to find how large Δt_o may be before $\overline{\Delta\phi(t)}$ due to Δt_o becomes too large to allow the required measurement accuracy. The function for $\overline{\Delta\phi(t)}$ indicates that the effect of Δt_o is greatest at larger t_o values and maximum for d/t_o minimum.

$$(Vt_o)_{max} \approx 3 \times 10^7 m$$

where

$$V = 5 \times 10^3 m/s,$$
$$d_{min} = 1.1 \times 10^7 m.$$

$\overline{\Delta L}$ = average value of change in range in meters

$$= \frac{\overline{\Delta\phi(t)}}{2\pi} \times \frac{CT}{2}$$

$$= \frac{V^2}{2L}\left(\frac{\Delta t_o^2}{3} + t_o \Delta t_o\right)$$

$$\overline{\Delta L}_{max} \cong \frac{V^2 t_o \Delta t_o}{2L}$$

$$\cong \frac{3.08 \times 10^7 \times 5 \times 10^3 \Delta t_o}{8.6 \times 10^7}$$

$$\cong 1.79 \times 10^3 \Delta t_o$$

$$= 50 \text{ km for } \Delta t_o = 28 \text{ seconds}$$

$$= 14.3 \text{ km for } \Delta t_o = 8 \text{ seconds}$$

Thus, the maximum error due to the 8-second integration is 14.3 km. Trajectory information yielding knowledge of t_o will further reduce error.

Note that when $t_o \approx 0$, the range variation is much less sensitive to Δt_o and is maximum at minimum sounding range when $L = 1.1 \times 10^7$.

Then

$$\overline{\Delta L} \cong \frac{V^2 \Delta t_o^2}{6L} \quad \text{when } t_o \approx 0$$

$$\cong \frac{25 \times 10^6 \Delta t_o^2}{6.6 \times 10^7}$$

$$\cong 3.79 \times 10^{-1} \Delta t_o^2$$

$$= 50 \text{ km for } \Delta t_o \cong 365 \text{ seconds.}$$

3. MODULATION DOPPLER SHIFT

The modulation sunusoid will have an instantaneous doppler shift equal to $\delta\phi(t)/dt$.

From paragraph 2,

$$\tau = \frac{2 \left[\sqrt{(Vt)^2 + d^2} - R \right]}{C}$$

$$\phi(t) = \frac{\tau}{T} \times 2\pi$$

$$= \frac{4\pi}{T} \left[\frac{\sqrt{(Vt)^2 + d^2} - R}{C} \right]$$

The instantaneous modulation frequency is $\delta\phi(t)/dt$.

$$\frac{\delta\phi(t)}{dt} = \frac{4\pi}{TC} \times \frac{1}{2} \frac{2V^2 t}{\left[(Vt)^2 + d^2\right]^{1/2}}$$

$$= \frac{4\pi}{TC} \frac{V}{\sqrt{1 + \left|\frac{d}{Vt}\right|^2}} \text{ cps}$$

B-6

Thus, function is maximum when (d/Vt) is minimum at maximum sounding range.

Let

$$T = \frac{1}{150}$$

$$V = 5 \times 10^3$$

$$C = 3 \times 10^8$$

$$\left(\frac{d}{Vt}\right)^2 = 1.95$$

$$\left[\frac{\delta\phi(t)}{dt}\right]_{max} = 1.83 \times 10^{-2} \text{ cps, which is maximum modulation doppler shift.}$$
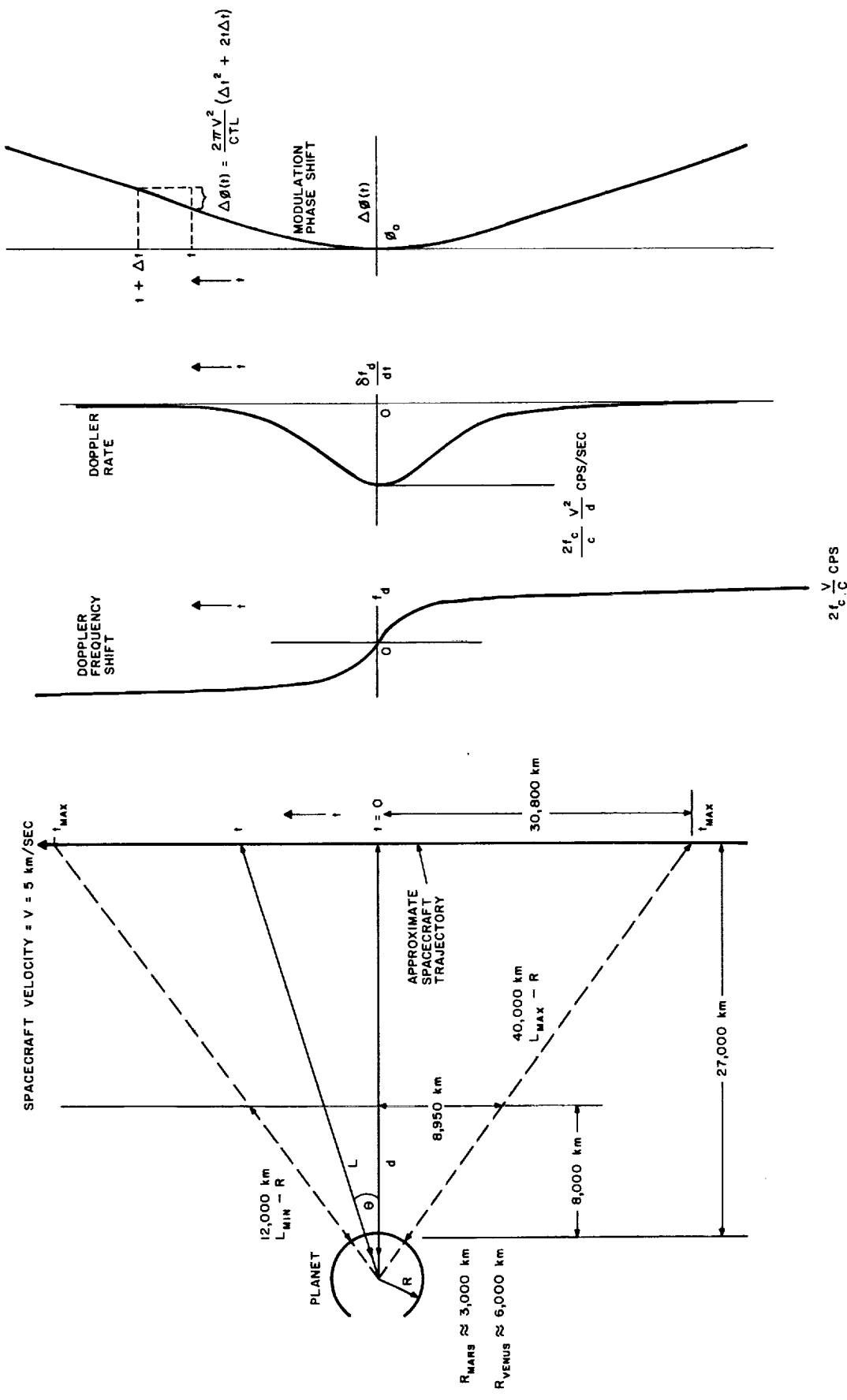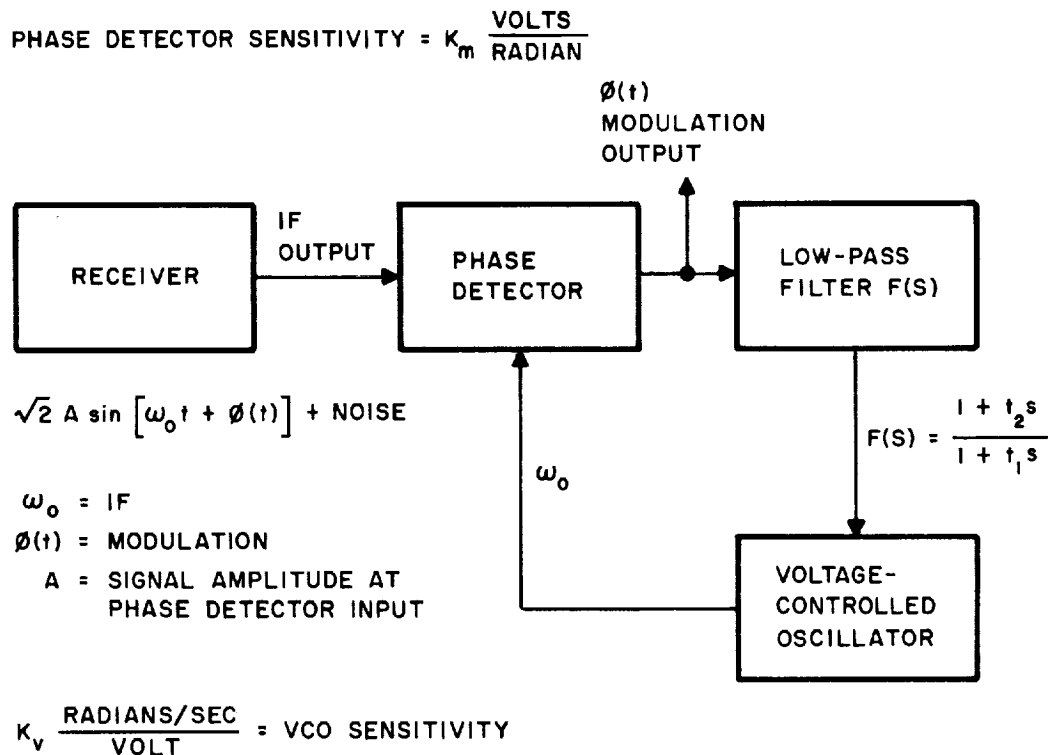
For $T = \frac{1}{150}$ seconds.

FIGURE B-1. SIGNAL VARIATIONS DUE TO SPACECRAFT MOTION

APPENDIX C
PHASE-LOCK LOOP PARAMETERS

The following diagram shows the phase-lock loop with its important design parameters.

PHASE DETECTOR SENSITIVITY $= K_m \dfrac{\text{VOLTS}}{\text{RADIAN}}$

$\emptyset(t)$
MODULATION
OUTPUT

| RECEIVER | IF OUTPUT → | PHASE DETECTOR | → | LOW-PASS FILTER F(S) |

$\sqrt{2}\, A \sin\left[\omega_0 t + \emptyset(t)\right] + \text{NOISE}$

$F(S) = \dfrac{1 + t_2 s}{1 + t_1 s}$

ω_0

$\omega_0 = \text{IF}$

$\emptyset(t) = \text{MODULATION}$

$A = \text{SIGNAL AMPLITUDE AT PHASE DETECTOR INPUT}$

VOLTAGE-CONTROLLED OSCILLATOR

$K_v \dfrac{\text{RADIANS/SEC}}{\text{VOLT}} = \text{VCO SENSITIVITY}$
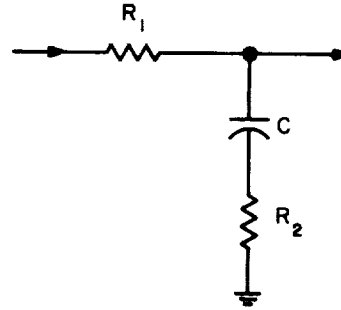
References 1 through 9 show various analyses of the loop and the optimum relationships between its parameters. The relationships that follow are for the optimization criterion of maintaining phase-lock with good transient response under the condition of a minimum input S/N.

The optimum low-pass filter for the desired second-order loop is

$$t_1 = (R_1 + R_2)C$$

$$t_2 = R_2 C$$

open-loop gain $= G = AK_m K_v$

3-db loop bandwidth (information bandwidth) $= B \frac{radians}{second}$

Two-sided noise bandwidth $= 2B_L \frac{radians}{second}$

Parameter values at threshold S/N of loop are indicated with subscript T.

The optimum relations are

$$B_T^2 = \frac{G_T}{t_1} = \frac{2}{t_2^2} \text{ for } t_1 \gg t_2$$

$$2B_{LT} = \frac{3\pi}{\sqrt{2}} B_T$$

Figure C-1 shows the dependence of 3-db loop bandwidth on loop-gain variations over the threshold value. Figure C-2 shows the phase shift in the detected modulation that results from the phase-lock loop as a function of the ratio of modulation frequency to loop 3-db bandwidth.

These relationships are important in that they indicate the effect of a varying S/N on the accuracy of measurements made of the phase of the demodulated signal.
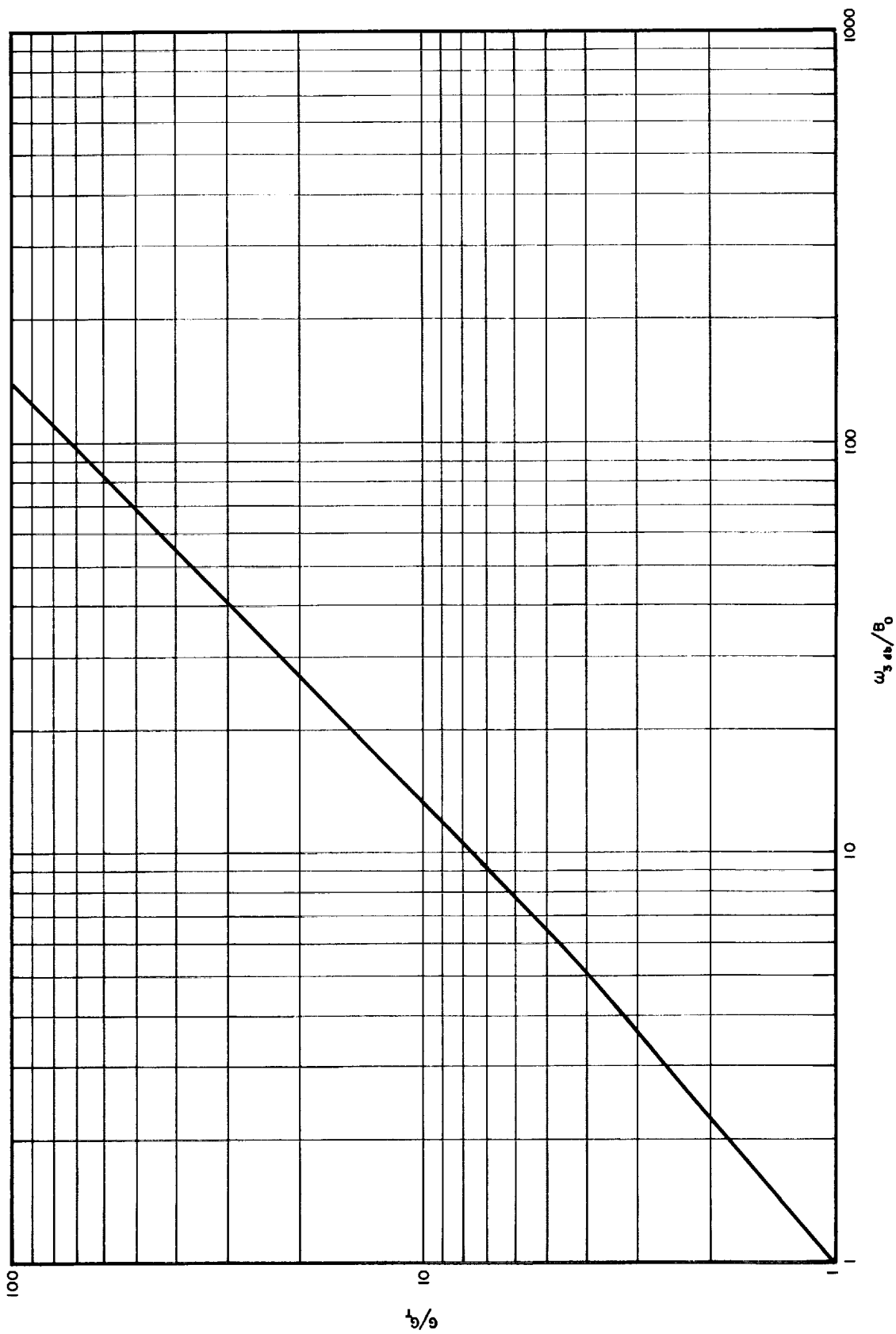
FIGURE C-1. VARIATION OF LOOP 3-DB BANDWIDTH VS RATIO OF OPEN-LOOP GAIN, G, TO THRESHOLD GAIN G_T

The graph shows PHASE SHIFT IN DEGREES on the y-axis (0 to 90) versus $\dfrac{\omega_m}{\omega_{3\,db}}$ on the x-axis (1 to 100, logarithmic), with the formula:

$$|\theta| = \tan^{-1}\left|\frac{\sqrt{2}\,\dfrac{\omega_m}{\omega_{3\,db}}}{1 - \left(\dfrac{\omega_m}{\omega_{3\,db}}\right)^2}\right|$$
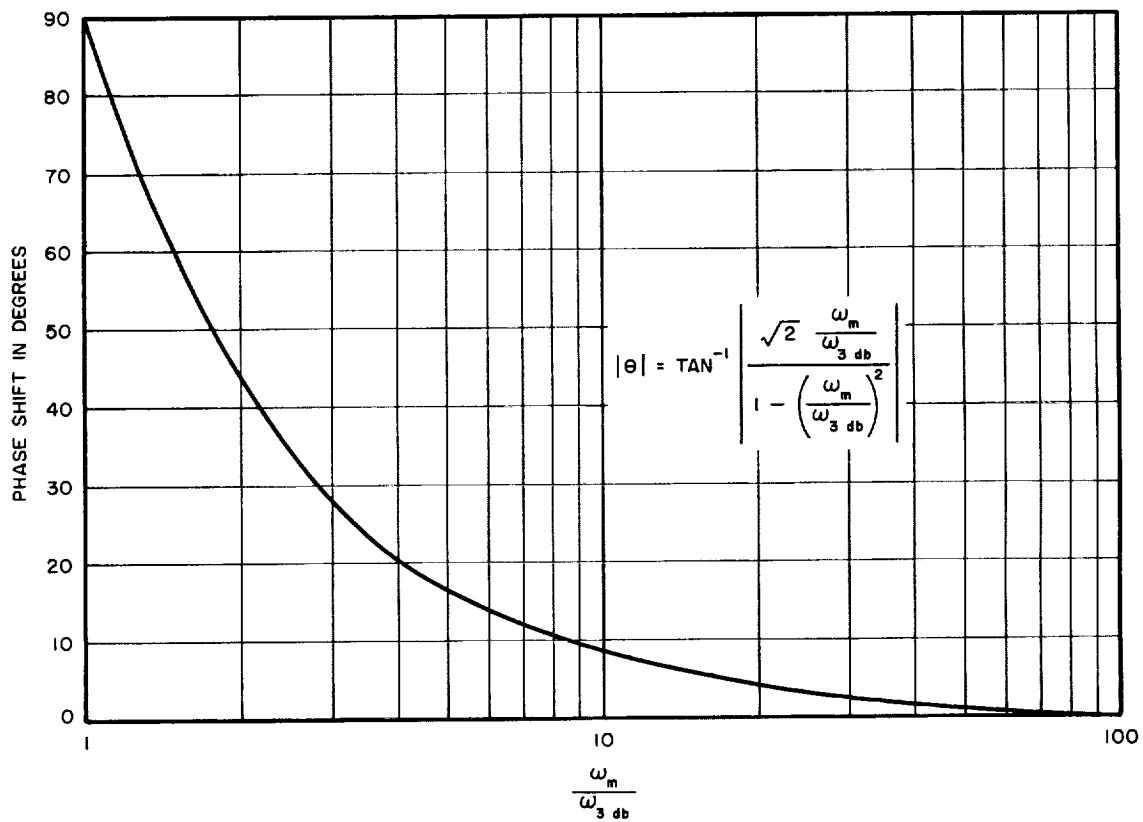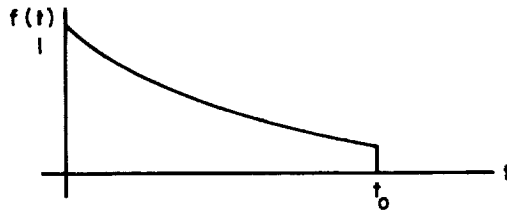
FIGURE C-2.   MODULATION PHASE SHIFT, θ, VS RATIO OF MODULA-
TION FREQUENCY TO PHASE-LOCK LOOP 3-DB BANDWIDTH

APPENDIX D
ANALYSIS OF RC INTEGRATOR

Given a filter with impulse response of:

$$f(t) = e^{-t/RC} \quad 0 < t < t_0$$
$$0 = \text{ELSEWHERE}$$

The equivalent noise bandwidth ω_n is

$$\omega_n = \int_0^\infty \frac{|F(\omega)|^2}{|F(o)|^2} \, d\omega \qquad (D\text{-}1)$$

where $F(\omega)$ is Fourier transform of $f(t)$ and filter input noise is white Gaussian. From Parseval's theorem:

$$\int_{-\infty}^\infty |F(\omega)|^2 \, d\omega = \frac{1}{2\pi} \int_{-\infty}^\infty f^2(t) \, dt \qquad (D\text{-}2)$$

Also, since $|F(\omega)|$ is even for real $f(t)$

$$\int_{-\infty}^\infty |F(\omega)|^2 \, d\omega = 2 \int_0^\infty |F(\omega)|^2 \, d\omega \qquad (D\text{-}3)$$

Then

$$\omega_n = \frac{1}{2\pi \, x |F(o)|^2} \, x\frac{1}{2} \int_{-\infty}^\infty f^2(t) \, dt \qquad (D\text{-}4)$$

$$w_n = \frac{1}{4\pi \ |F(o)|^2} \int_{-\infty}^{\infty} f^2(t) \ dt \qquad (D-5)$$

$$f^2(t) = e^{-2t/RC} \ \bigg|_{t = 0}^{t = t_o} \qquad (D-6)$$

$$\int_o^{t_o} e^{-2t/RC} \ dt = -\frac{RC}{2} \left[e^{-2t_o/RC} - 1 \right] \qquad (D-7)$$

and

$$w_n = \frac{RC}{8\pi \ |F(o)|^2} \left[1 - e^{-2t_o/RC} \right] \qquad (D-8)$$

Taking the Fourier integral:

$$F(w) = \frac{1}{2\pi} \int_{-\infty}^{\infty} f(t) \ e^{-jwt} \ dt \qquad (D-9)$$

$$= \frac{1}{2\pi} \int_o^{t_o} e^{-t(1/RC+wj)} \ x \ dt \qquad (D-10)$$

$$F(w) = \frac{1}{2\pi} \ \frac{-1}{\frac{1}{RC} + jw} \left[e^{-t_o(1/RC+jw)} - 1 \right] \qquad (D-11)$$

$$F(o) = -\frac{RC}{2\pi} \left[e^{-t_o/RC} - 1 \right] \qquad (D-12)$$

Substituting $|F(o)|^2$ in equation D-8

$$\omega_n = \frac{RC}{8\pi} \times \frac{4\pi^2}{(RC)^2} \frac{1 - e^{-2t_o/RC}}{(1 - e^{-t_o/RC})^2} \qquad (D-13)$$

$$\omega_n = \frac{\pi}{2RC} \frac{1 + e^{-t_o/RC}}{1 - e^{-t_o/RC}} \qquad (D-14)$$

An ideal integrator is approximated by $t_o/RC \ll 1$: then

$$\omega_n^1 \cong \frac{\pi}{2RC} \frac{2 - (t_o/RC)}{(t_o/RC)} \qquad (D-15)$$

$$\omega_n^1 \cong \frac{\pi}{t_o} \qquad\qquad f_n = \frac{\omega_n}{2\pi}$$
$$\qquad\qquad\qquad (D-16)$$
$$f_n^1 = \frac{1}{2t_o}$$

Let R = ratio of ω_n to ideal integrator of bandwidth ω_n^1. Then

$$R = \frac{t_o}{2RC} \frac{1 + e^{-t_o/RC}}{1 - e^{-t_o/RC}} \qquad (D-17)$$

Tabulating R versus t_o/RC

t_o/RC	R (db)	
1/4	1.005	= 0.05
1/2	1.02	= 0.1
1	1.08	= 0.3
2	1.30	= 1.1
4	2.07	= 3.2
6	3.01	= 4.8

APPENDIX E

MODIFICATION OF RANGING TECHNIQUE TO
MINIMIZE AMBIGUITIES

1.   PROBLEM

        Measurement of the phase shift of a single modula-
tion tone for ranging requires a compromise between range
resolution and maximum nonambiguous range. This is due to
the angular resolution limitation associated with the S/N
(Appendix A). The compromise is minimized by the use of more
than one modulation tone. A procedure such as this may pro-
vide a practical solution to the absolute altimetry problem,
though this problem is not analyzed in detail.

2.   USE OF TWO TONE MEASUREMENTS

        The problem may be solved with two different modu-
lation tones, by performing two range measurements with equal
angular resolution. One range measurement using the 150-cps
tone would provide the 50-km resolution within a 1000-km band.
The second measurement, with equal S/N, would define 1000-km
range increments within a 20,000-km band. This combination
defines a 50-km element within a 20,000-km nonambiguous inter-
val.

        The problem encountered in using this concept in the
sounder is that the coarse ranging tone would be 7-1/2 cps.
This frequency, though outside the 3-db frequency of the phase-
lock look, would still be subject to significant phase shift
and resultant measurement uncertainty due to the presence of
the loop.

3. VERNIER TECHNIQUE

A vernier technique using two tones of similar frequency will also reduce the measurement ambiguity. Let:

D = Maximum nonambiguous sounding range,

R = Sounding range,

f_1 = Tone frequency 1,

f_2 = Tone frequency 2,

C = Average velocity of propagation (about 3×10^8 m/sec),

Θ_1 = Measured phase delay of f_1,

Θ_2 = Measured phase delay of f_2.

Let:

$$\lambda_1 = \frac{C}{f_1}$$

$$\lambda_2 = \frac{C}{f_2} \qquad \text{and let} \qquad \lambda_1 > \lambda_2$$

Let:

$$\frac{2D}{\lambda_1} = n_{max} \qquad \text{and} \qquad \frac{2D}{\lambda_2} = n_{max} + 1$$

and n is an integer representing the number of ambiguities in sounding range D with one tone.

$$\frac{2R}{\lambda_1} = n + \frac{\Theta_1}{2\pi}$$

$$\frac{2D}{\lambda_1} = n_{max} \qquad \text{and} \qquad \frac{2D}{\lambda_2} = n_{max} + 1$$

Then:

$$\frac{2D}{\lambda_2} = \frac{2D}{\lambda_1} + 1$$

$$2D = \frac{1}{1/\lambda_2 - 1/\lambda_1}$$

$$2D = \frac{C}{f_2 - f_1}$$

Thus, to perform nonambiguous range measurements over a 40,000-km distance ($D = 4 \times 10^7$) using one tone at 150 cps ($f_1 = 150$) requires that

$$f_2 = \frac{C}{2D} + f_1$$

$$= \frac{3 \times 10^8}{4 \times 10^7 \times 2} + 150$$

$$f_2 = 153.75 \text{ cps}$$

The nonambiguous range is obtained as follows. For $(\Theta_2 - \Theta_1) > 0$:

$$\frac{R}{T_2} = n + \frac{\Theta_2}{2\pi}$$

and

$$R = \frac{\Theta_2 - \Theta_1}{2\pi} \left(\frac{C}{f_2 - f_1} \right)$$

$$R = \frac{\Theta_2 - \Theta_1}{2\pi} D \text{ for } (\Theta_2 - \Theta_1) > 0$$

for $(\Theta_2 - \Theta_1) < 0$

$$\frac{R}{T_2} = (n + 1) + \frac{\Theta_2}{2\pi}$$

and

$$R = \left[1 - \left(\frac{\Theta_1 - \Theta_2}{2\pi} \right) \right] \frac{C}{f_2 - f_1}$$

$$R = \left[1 - \left(\frac{\Theta_1 - \Theta_2}{2\pi} \right) \right] D \text{ for } (\Theta_2 - \Theta_1) < 0$$

4. DEPENDENCE ON S/N

The resolution in R that can be obtained is limited by the S/N and its effect on the resolution of Θ (Appendix A). For $(\Theta_2 - \Theta_1) > 0$

$$R = \frac{\Theta_2 - \Theta_1}{2\pi} \times D$$

If $(\Theta_2 - \Theta_1)$ has an uncertainty of $\Delta\Theta$, this will cause an uncertainty in R of ΔR. Thus,

$$R + \Delta R = \frac{(\Theta_2 - \Theta_1) + \Delta\Theta}{2\pi} \times \frac{c}{f_2 - f_1}$$

$$\Delta R = \frac{\Delta\Theta}{2\pi} \times \frac{c}{f_2 - f_1}$$

$$\frac{\Delta R}{R} = \frac{\Delta\Theta}{(\Theta_2 - \Theta_1)}$$

Thus, the percent range resolution is the same as that of the phase angle and is similarly affected by S/N.

5. DEPENDENCE ON FREQUENCY ACCURACY

The range accuracy is affected by the accuracy of $(f_2 - f_1)$. An error ΔR in range will result from an error Δf in $(f_2 - f_1)$.

$$R + \Delta R = \frac{\Theta_2 - \Theta_1}{2\pi} \frac{c}{[(f_2 - f_1) + \Delta f]}$$

$$\frac{\Delta R}{R} = \frac{-\Delta f}{(f_2 - f_1) + \Delta f}$$

Thus, percent range accuracy is about the same as $(f_2 - f_1)$ accuracy for small errors.

APPENDIX F
RF SIGNAL GENERATION STABILITY

1. ## STABILITY OF SINGLE OSCILLATOR

The following is a derivation of the frequency stability required by a crystal oscillator driving two fractional frequency multipliers (Figure F-1) whose difference must be kept to a given tolerance:

Let

f_1 = Output frequency of crystal-controlled oscillator,

C_1 = Fractional change in frequency f_1,

K_1 = Fractional change in frequency in fractional frequency multiplier number one,

K_2 = Fractional change in frequency in fractional frequency multiplier number two.

The deviation in the difference of the outputs of the two fractional multipliers is caused by a fractional change in f_1 of C is equal to:

$$C_D = \frac{(K_2 f_1 - K_1 f_1) - \left[K_2(f_1 + Cf_1) - K_1(f_1 + Cf_1) \right]}{K_2 f_1 - K_1 f_1}$$

$$= \frac{f_1(K_2 - K_1) - f_1(K_2)(1 + C) + K_1(f_1)(1 + C)}{f_1(K_2 - K_1)}$$

$$C_D = -C$$

Thus, a fractional change in frequency f_1 will produce an equal fractional change in the difference of the outputs of the fractional frequency multipliers.

2. STABILITY OF TWO SEPARATE OSCILLATORS

The following is a derivation of the frequency stability required by the two crystal oscillators shown in Figure 10-1.

Let:

F_A = Frequency of receiver oscillator,

F_B = Frequency of transmitter oscillator,

C_A = Fractional frequency change of oscillator F_A,

C_B = Fractional frequency change of oscillator F_B.

The deviation in the difference of the two oscillators for given changes in the oscillators is equal to:

$$C_D = \frac{F_B - F_A - \left[(F_B + C_B F_B) - (F_A + C_A F_A) \right]}{F_B - F_A}$$

$$= \frac{C_A F_A - C_B F_B}{F_B - F_A}$$

In the worst case $C_B = -C_A$

Then:

$$C_D = C_A \left(\frac{F_A + F_B}{F_B - F_A} \right)$$

When

$$F_A = 21 \text{ Mc and } F_B = 17.5 \text{ Mc}$$

Then

$$C_D = 11 C_A$$

Thus, in the worst case, an equal but opposite fractional change in the oscillators will cause a fractional change in the difference to be greater by a factor of 11.

| BUFFER AMPLIFIER | → | 1/5 FRACTIONAL FREQUENCY MULTIPLIER | 5.25 Mc | PHASE MODULATOR | → | X4 MULTIPLIER | → | 21-Mc OUTPUT TO TRANSMITTER MIXER |

STARTER CIRCUIT

26.25-Mc CRYSTAL OSCILLATOR

STARTER CIRCUIT

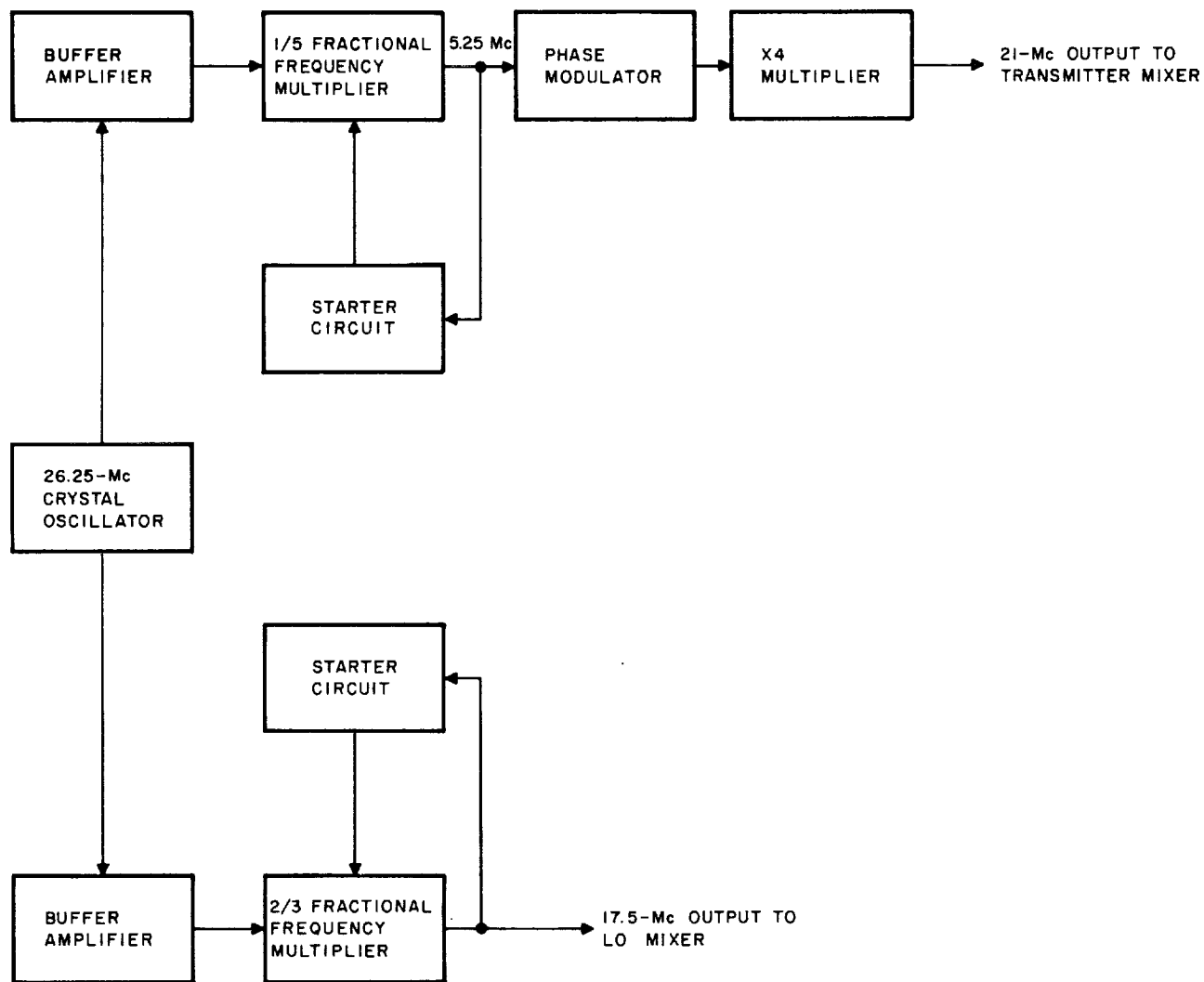BUFFER AMPLIFIER → 2/3 FRACTIONAL FREQUENCY MULTIPLIER

17.5-Mc OUTPUT TO LO MIXER

FIGURE F-1.   FRACTIONAL FREQUENCY MULTIPLIER PLAN OF RF GENERATION